M 2019

FEUP FACULDADE DE ENGENHARIA
UNIVERSIDADE DO PORTO

Hysteresis in Tire Textile Reinforcements focusing on PET material

ANDRÉ BILTES DE SOUSA CARDOSO
DISSERTAÇÃO DE MESTRADO APRESENTADA
À FACULDADE DE ENGENHARIA DA UNIVERSIDADE DO PORTO EM
ÁREA CIENTÍFICA

INTEGRATED MASTER IN CHEMICAL ENGINEERING

Hysteresis in Tire Textile Reinforcements focusing on PET material

A Master's dissertation

of

André Cardoso

Developed within the course of dissertation

held in

Continental AG / Body Compound & Reinforcement Technology Department

Supervisor at FEUP: **Prof. Fernão Magalhães**

Supervisor at Continental: **Dr. Thomas Kramer**

U.PORTO

FEUP FACULDADE DE ENGENHARIA
UNIVERSIDADE DO PORTO

Departamento de Engenharia Química

February of 2019

CONFIDENTIAL DOCUMENT. USE ONLY FOR EVALUATION PURPOSES

This master's thesis contains confidential information from Continental Reifen Deutschland GmbH. Duplication or distribution of the work, as well as the utilization or communication of its contents, is strictly prohibited without the express written authorization of Continental Reifen Deutschland GmbH, Jädekamp 30, 30419 Hanover.

Acknowledgements

First, I would like to acknowledge the Department of Chemical Engineering of Faculty of Engineering, University of Porto and the Continental Reifen Deutschland GmbH for all the conditions provided for the development of my Master Thesis. At this point, I would like to thank everyone for the support and assistance which was given to me during my employment and the development of this work. I am also truly grateful to:

- Dr. Thomas Kramer, for his availability, constant support and invaluable advice; and for the chance to explore such an inspiring topic, allowing me to discover the potential of R&D. Prof. Fernão Magalhães, for his helpful feedback and his guidance.

- Everyone in the R&D Department, but especially Tiago Moura, Daniel Pinho, Miguel Bispo and Nermeen Nabih, for always making me feel welcome, as well as for all the friendly advice and support.

- Anuwat Suwannachit, Christian Neufeld and Andreas Maibohm, for including me in the team and for always being available to help.

- My family and friends, for keeping me company from miles away, for always being there when I needed a word of support, but especially for always believing in me.

This work was funded by Continental Reifen Deutschland GmbH and by project POCI-01-0145-FEDER-006939 (Laboratory for Process Engineering, Environment, Biotechnology and Energy - UID/EQU/00511/2013) funded by the European Regional Development Fund (ERDF), through COMPETE2020 - Programa Operacional Competitividade e Internacionalização (POCI) and by national funds, through FCT - Fundação para a Ciência e a Tecnologia.

Abstract

The pneumatic tire is one of the main important elements of a vehicle with a high level of complexity. It is constituted by several materials and components and must comply with the vehicle requirements. One of the materials that is responsible to fulfil these requirements are textile reinforcing materials. These materials experience a phenomenon called hysteresis, which is the main contributor to rolling resistance, leading to an increase of fuel consumption. Thus, hysteresis has been attracting the attention of researchers and suppliers, being the motivation of several recent studies, mainly for rubber, in order to reduce energy losses and fuel consumption.

In the present thesis the aim was to investigate textile reinforcements with focus on Polyethylene terephthalate (PET) and its hysteresis properties dependence on temperature, frequency, static pre-deformation and strain amplitude. To have a better understanding of the PET material properties both stepwise relaxation and dynamic tests were performed, respectively with Zwick / Roell and MTS Acumen 3 testing machines.

Temperature influenced the material properties of textile reinforcement´s cords. The textile cords tested experienced softening with increase of temperature; and stiffened with increase of strain. Thermal polymer transitions seemed to influence the textile cords modulus response to stress. The amount of hysteresis seems to increase with pre-deformation and strain amplitude. The stiffness increased with pre-deformation and decreased with strain amplitude. Temperature monitoring of cord constructions of PET 1400x2 and Nylon 2800x2 cords disclosed more variation and higher peak of temperature and more amount of hysteresis when compared with their respective lower material constructions- PET 630x2 and Nylon 940x2. Throughout these tests the amount of hysteresis decreased for all material constructions tested. Noteworthy, different dynamic tests show similar results in similar conditions, which may be a good indicator of the replicability of the tests. It was also obtained a master curve, by evaluating the modulus variables as a function of frequency and temperature. Taken as a whole, despite specific limitations, this project allowed for a better understanding of the behavior of some textile reinforcements used in pneumatic tires under both static and dynamic conditions, as well as the analysis of hysteresis influencing factors.

Keywords: textile reinforcement cords, hysteresis, viscoelasticity

Resumo

O pneu é um dos elementos mais importantes de um veículo e tem um alto nível de complexidade. É constituído por vários materiais e componentes e deve cumprir com os requisitos do veículo. Um dos materiais responsáveis para atingir esses requisitos é o reforço têxtil. Esses materiais apresentam um fenômeno de histerese, que é o principal contribuinte para a resistência ao rolamento e leva a um incremento no consumo de combustível. Assim, a histerese tem atraído a atenção de investigadores e fornecedores, sendo a motivação de vários estudos recentes, principalmente relacionados com a borracha, a fim de reduzir as perdas de energia e minimizar o consumo de combustível.

Na presente tese, o objetivo foi investigar reforços têxteis com foco no Polietileno Tereftalato (PET) e as suas propriedades de histerese, dependentes da temperatura, frequência, pré-deformação estática e amplitude de deformação. Para uma melhor compreensão das propriedades do PET, foram realizados tanto o relaxamento passo-a-passo como testes dinâmicos, respectivamente, com as máquinas de teste Zwick / Roell e MTS Acumen 3.

A temperatura influenciou as propriedades do material das cordas de reforço têxtil. As cordas têxteis testadas sofreram aumento da maleabilidade com o aumento da temperatura; e endurecimento com o aumento da tensão. As transições térmicas de polímeros parecem influenciar a resposta do módulo das cordas têxteis ao stresse. A quantidade de histerese parece aumentar com a pré-deformação e a amplitude de deformação. A rigidez aumentou com a pré-deformação e diminuiu com a amplitude de deformação. A monitorização da temperatura das cordas têxteis de PET 1400x2 e Nylon 2800x2 revelou maior variação e maior pico de temperatura, assim como maior quantidade de histerese quando comparado com as respectivas construções de materiais com menor densidade - PET 630x2 e Nylon 940x2. Durante estes testes, a quantidade de histerese diminuiu em todas as construções de material testadas. Note-se que, diferentes testes dinâmicos revelaram resultados semelhantes em condições idênticas, o que pode ser um bom indicador da replicabilidade dos testes. Também foi obtida uma curva mestra, avaliando as variáveis de módulo em função da frequência e da temperatura. Globalmente, apesar de limitações específicas, este projeto permitiu um melhor entendimento do comportamento de alguns reforços têxteis utilizados nos pneus sob condições estáticas e dinâmicas, bem como a análise de fatores que influenciam a histerese.

Palavras Chave: corda de reforço têxtil, histerese, viscoelasticidade

Declaration

I hereby declare, on my word of honor, that this work is original and that all non-original contributions were properly referenced with source identification.

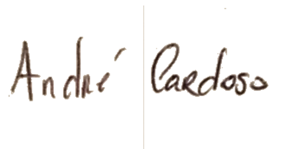

February of 2019

Contents

List of Figures

List of Tables

Notation and Glossary

ε	Strain	%
σ	Stress	N mm^2
σ_{vis}	Overstress	N mm^2
σ_{∞}	Equilibrium stress	N mm^2
F	Force	N
t	Time	h
T	Temperature	° C
RT	Room temperature	° C
ω	Frequency	Hz
E’	Storage modulus	N mm^2
E’’	Loss modulus	N mm^2
δ	Phase lag	°
tan δ	Loss factor	
TF	Twist factor	
LD	Linear density	dtex
α_T	Shift factor	

List of Acronyms

R&D	Research and Development.
PET	Polyethylene terephthalate.
DMA	Dynamic Mechanical Analysis.
TTS	Time Temperature Superposition.
MPT	MultiPurpose Testware.
MPE	MultiPurpose Elite.
DIN	Deutsches Institut für Normung.

1 Introduction

1.1 Framing and presentation of the work

This master thesis has been developed according to the requirements for the degree of Master of Chemical Engineering and its subject theme addresses hysteresis in tire textile reinforcements focusing on polyethylene terephthalate (PET) material. This work was only achievable due to the collaboration between Continental and University of Porto.

The focus of this thesis is the study the PET cords and some of its hysteresis properties under static and dynamic conditions.

1.2 Continental AG

Continental was founded in Hannover in 1871 as the stock corporation “Continental-Caoutchouc- und Gutta-Percha Compagnie”. Manufacturing at the main factory in Hannover included soft rubber products, rubberized fabrics, and solid tires for carriages and bicycles. (1)

Continental Corporation is divided in two groups, the Automotive Group and the Rubber Group, and consists of 5 divisions: Chassis & Safety, Powertrain, Interior, ContiTech and Tires and employs about 240 000 people, operating at 554 locations in 60 countries. (2) Continental has shown commitment in innovation and progress for more than 145 years while developing technologies, systems, and service solutions that make mobility and transport more sustainable, safer, more comfortable, more customized, and more affordable.” (3)

As a supplier of brake systems, systems and components for powertrains and chassis, instrumentation, infotainment solutions, vehicle electronics, tires and technical elastomers, Continental contributes to enhanced driving safety and global climate protection. Continental is also a reference partner in networked automobile communication. (1)

1.3 Contributions of the work

Parameters such as temperature, frequency, static pre-deformation and strain amplitude were evaluated in the experiments of this thesis.

The main contribution of this thesis was the validation and implementation of both static and dynamic test methods that allowed the determination and evaluation of the viscoelastic and hysteresis properties in textile reinforcements, focusing on PET material. Also, it adds in a new test procedure for textile reinforcement cords, which allowed the evaluation of the temperature cords under dynamic conditions.

This thesis considered the work done by Mariana Gomes, which studied under dynamic conditions the hysteresis properties of Nylon 6.6 cord reinforcements assessed by the influence of temperature, frequency, linear density and twist. PET cords were also used to evaluate the influence of the dip pick up percentage (DPU %). Gomes thesis work main conclusions were: (4)

1. Twist indicated a negatively linear effect on the storage and loss moduli, presenting a negligible change for the overall damping capacity. (4)

2. For linear density, characteristic variables indicated curvature, entailing further studies to settle their specific effect. (4)

3. DPU % indicated a very small impact on the hysteresis of the cords, only presenting a statistically significant effect for the storage modulus, following a negative linear correlation. Besides that, microscopy analysis of the cords' cross-sections revealed no evidence of a difference in the dip penetration. (4)

1.4 Organization of the thesis

This master thesis is divided into 8 sections briefly described as follows:

1. Introduction exposes an overview of the developed work and its importance to Continental AG.

2. Context and State of the art presents the current knowledge on the modern tire, textile reinforcements, and rolling resistance, as well as a brief introduction to viscoelasticity and hysteresis.

3. Material and Methods describes the equipment and testing methodology used in this study.

4. Results and Discussion include a display of the obtained results and their evaluation.

5. Conclusions presents a brief review of the results and the main assumptions of the thesis.

6. Assessment of the work done consists of a critical analysis of the developed work, mentioning achieved accomplishments and suggestions for further study.

References lists all the sources referred throughout the thesis.

Appendix include some complementary information expected to follow the work elaboration of this thesis.

2 Context and State of art

2.1 Overview of the modern tire

Tires are the interface reaction point of the vehicle with the path (e.g. road) and they must cope with impacts and disturbances and respond to them.

Tires transfer the forces that hail from the driver´s commands directly onto the road. Longitudinal forces arise during acceleration and braking, and lateral forces are given by cornering. When cornering both lateral and longitudinal forces share the forces transmitted to the road. The tire performance has to comply with the vehicle requirements, particularly when it comes to, not only cornering, but also accelerating or braking. These requirements must be certified in every surface condition; even when the path is wet, with snow or ice.

It is well-defined nowadays that tires have an important role in motor cars and that they hold some challenges to overcome. Not only tires need directional stability but also need to have an adequate load capacity, damping performance, contact patch with the road and grip. (5)

The construction of tires was the result of a long evolutionary process, which was driven by the growing necessity for comfort, mileage, force transmission and speed. To fulfil these requirements, tires need to be simultaneously flexible and stiff. Flexibility and stiffness are achieved not only by the construction itself, but also by the materials that comprise tires. (5)

2.2 Materials and components used in tires

Reinforcers such as steel and textile are part of the materials of passenger car tires.” (6) The typical PLT materials distribution mainly consists of rubber, steel and textile as shown in Figure 1.

Figure 1 - Reinforcement materials in a PLT tire (5)

The construction of pneumatic tires has not changed significantly throughout the years and mainly consists of tube, carcass, tread and bead. These and more components are shown in Figure 2.

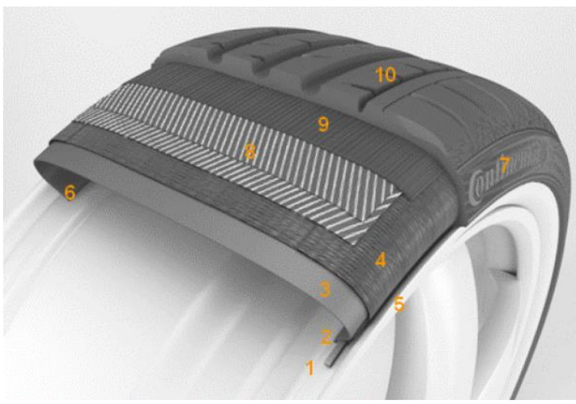

Figure 2 – Components in a PLT tire (7)

The main components that make up a PLT tire are descripted in Table 1.

Table 1 – Materials of PLT tire components and their main functions. (8)

#	Component	Material	Main functions
4	Carcass	PET and rayon	Ensures load capacity
5	Bead	Steel cords	Holds the tire in its place on the rim
8	Belt	Steel cords	Reduces movement of tread blocks between tread and road
9	Cap ply	Nylon and aramid	Reduces tire growth
10	Tread	Rubber	Ensures grip

Further tires components and their functions in more detail can be found in Appendix A.

The belt is one of the main components of PLT. The belt makes the tire stiffer, which led to less wear. At the same time a stiffer tire transfers more forces onto the road, and so improves its handling performance. The stiffness of the belt results from steel, which is strong and fatigue resistant at the same time. Apart from steel, passenger car tires contain a further reinforcing material: textile. (5) (9) (10)

2.3 Textile reinforcements

Different textile materials are used depending on the function of the component. While the carcass generally consists of polyester or rayon, the selected materials for the cap ply are usually nylon and aramid. (11)

2.3.1 Carcass textiles: PET and rayon

Different textiles display different elongation characteristics. In this regard, polyester and rayon are considered the most suitable textiles for the carcass. Despite their different modulus, they are both simultaneously flexible and tear-resistant. (12) (13)

Carcass made from polyester reliably serves its purpose in everyday conditions. Rayon is a synthetic fiber of cellulose and it is notably more expensive. Its storage is challenging, as rayon displays a high tendency to absorb water and once the critical level is exceeded, this will lead to a reduced modulus and thus less tire stiffness. To avoid this deterioration in handling performance, rayon has to be stored under climate control. (14) (12) (13) (15)

2.3.2 Cap ply textiles: nylon and aramid

At high speed, passenger car tires without cap ply may certainly start to grow, due to huge centrifugal forces. This tire growth reduces the contact path and consequently, less force can be transmitted onto the road. However, a cap ply solves this difficulty.

The cap ply bundles and constricts, which stiffens the tire in general, keeping the force transmission and handling performance at its high level. Altogether, the cap ply hedges the centrifugal forces and thus limits the tire growth. These helpful wanted effects are achieved by the special properties of the cap ply materials: nylon and aramid.

Nylon is a synthetic polyamide, which brings together some unique features: it is even more tear-resistant and flexible than polyester and rayon. Nylon also shrinks when heated and does not revert to its initial state. For the cap ply, by contrast, shrinking nylon is a most convenient for a good reason: (14) with increasing speed, a moving tire warms progressively. What happens then is that the nylon natural response is to shrink but this shrinkage is prevented by the surrounding rubber. This prevented shrinkage leads to a force: the residual shrinkage force, which counteracts the centrifugal force, and prevents tire growth. Up to a certain speed, a cap ply made from nylon would work perfectly well. For very high-speed conditions however this may not be acceptable, and the tire has to become stiffer. To improve this issue, another material is added: aramid.

Like nylon, aramid is a synthetic fiber made from polyamides. While nylon is flexible, aramid is a very stiff material with low weight. The stiffness of aramid may raise a problem of processing during the tire building which requires at least a minimum degree of cord elongation. Regrettably, aramid is so stiff, that it hardly lengthens. Thus, aramid has to be softened somehow to make it processible. (14)

The flexibility of nylon is the key to this softening. By twisting aramid and nylon cords together, the outcome is a hybrid cord. This hybrid is flexible enough to enable the tire building process and also strong enough to ensure stiffness at high-speed. Thus, the hybrid cord combines the force-elongation behavior of nylon at low forces during the tire building process with the superior stiffness of aramid at high forces which occur under high-speed conditions. A more detailed description of the materials mentioned can be found in Appendix A.

2.4 Cord design and properties of textiles

As described in Chapter 2.2, the carcass' main contribute to the key requirements is the force transmission; in addition, there is also comfort and shock absorption. Each time the tire passes through the contact patch, the carcass is periodically stretched and released. Accordingly, carcass materials have to be robust, durable and at the same time flexible. Therefore, a crucial feature of the tire textiles is their elongation behaviour.

Elongation is only reversible to a certain extent, which then would lead to material fatigue and reduced mileage. Yet, it is possible to delay material elongation and protect the material by adding to it another structure. This structure consists of filaments piled together to yarns and these yarns twisted to form a cord. If these cords are twisted and then submitted to a force, the structure elongates before the material itself must. This structural elongation is reversible and protects the material until a specific degree. Only after submitting to a further increase of force, the structure may reach its limits and the material starts to elongate. Textiles chosen for the carcass should ensure that ordinarily purely structural elongation takes place, while material elongation should only occur under remarkable situations such as sudden impacts.

For the cord construction understanding there are several process stages.
Spinning – assembling of filaments into yarns. Usually, it is necessary to modify the yarn, in order to obtain the optimum benefit from their incorporation as reinforcement in elastomeric composites. (16)
Twisting – twisting of yarns to obtain a cord. (17) (16)
Weaving – assemble the yarns or cords together into a coherent to construct a fabric. (18) (16)
Dipping - a treatment of the textile, usually with resorcinol formaldehyde resin, that creates an interface, which improves the adhesion, allowing the bonding between the cord and the rubber. (19) (16)
Calendaring - technique that combines textile and rubber. (14) (16)

The structural elongation potential increases with the amount of twists. Textiles used in the tire typically have a twist level of 200 to 400 tpm. Besides the twist level, the qualities of the textiles also depend on the number and diameter of the filaments, both making up the linear density.

The higher the density, the thicker and stronger the material turns out to be. The density of textiles used in tires ranges from 500 to 3000 dtex. The linear density is useful for the cord construction. Textile cords description is based on the individual density. The number of twisted yarns and density together define the cord construction.

Another correlation that is currently used is between the density and the twist level, calculated by the twist factor (TF), as shown in Equation 1.

$$TF = twist\ level \sqrt{\frac{Total\ cord\ density}{10000}} \qquad (1)$$

2.5 Hysteresis

2.5.1 Stress and strain

When a sinusoidal stress is applied to a viscoelastic material the outcome is, to a certain degree, a sinusoidal deformation and the force needed to do that depend on the mechanical properties of the material. This means that different materials may have different stiffness values. The ratio of stress to strain reveals the material´s characteristic stiffness, which can be evaluated as the value E'. This stiffness is so-called modulus of elasticity.

This modulus expresses a material´s resistance to deformation when a certain stress is applied. It is known that a stiffer material is expected to have higher modulus E', and vice-versa. This characteristic stress-strain can be observed in Figure 3.

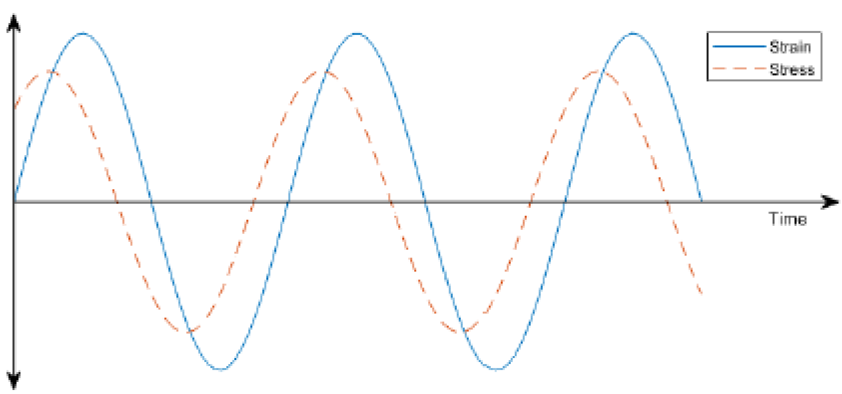

.

Figure 3 - Strain response to sinusoidal stress applied over time for a viscoelastic material (4)

The time shift in deformation leads to a translation along the x-axis and turns into a visible phase lag (δ). This lag is triggered by the inner friction of vulcanized polymer chains. It is always associated to an energy loss, the so-called dissipation. The whole phenomenon is known as hysteresis and is shown in Figure 4.

The amount of hysteresis depends on the phase angle of δ, and it is given by tan δ. Different compounds have different tan δ, presenting different degrees of dissipation when the compound gets deformed. Hence, tan δ measures the energy loss and it depends on the material composition, displaying different degrees of dissipation when the compound gets deformed. The degree of dissipation is influenced by the material´s internal damping, which in turn depends on its chemical composition.

The stress-strain pattern, represented in Figure 4, fits to a certain compound and displays its characteristic hysteresis properties. The larger the ellipse, the more energy gets dissipated. Accordingly, one compound with less hysteresis would lead to a smaller ellipse. (20)

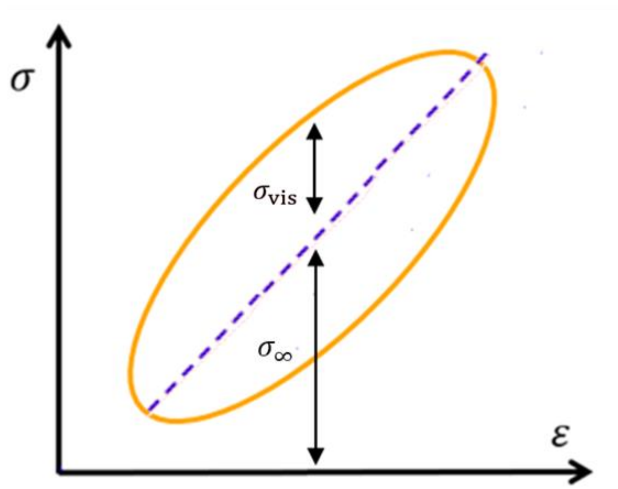

Figure 4 - Stress-strain plot behavior for viscoelastic materials

Stress can be described by the Equation 2.

$$\sigma(t) = \sigma_{\infty} + \sigma_{vis}(t) \quad (2)$$

For polymers such as textile reinforcement cords, the stress is dependent of two variables: a time independent , and a time-dependent variable . Time dependent behavior can be defined by the stress relaxation term, in which is applied a constant strain, and the response is measured in terms of a decrease in stress as a function of time as it will be addressed in Subsection 2.5.3. (22)

This hysteresis phenomenon goes together with energy dissipation but there is a good outcome of this energy loss that is associated with rolling resistance.

2.5.2 Rolling resistance

A rolling tire gets deformed over its entire length and width, creating a broad contact patch which advantageously swallows much of the road´s bumps and irregularities. (20)

This structural deformation occurs with each rotation. Nonetheless, once deformation occurs, heat starts to dissipate. This energy loss through repeated deformation is known as rolling resistance. (20)

Tire deformation → energy dissipation → rolling resistance

Rolling resistance is the energy consumed by a tire per distance unit. (21) It stands for a permanent energy loss and this energy comes from fuel. When riding on a highway in a passenger car, the tires´ share of the overall fuel consumption comes up to 20 percent; in inner-city traffic it is even as high as 30 percent. Predictably, the reduction of the rolling resistance became a persistent challenge and a major requirement in tire development

As hysteresis is connected to rolling resistance and is also crucial for braking, there is a target conflict - a high hysteresis for grip purposes versus a low rolling resistance compound with little hysteresis and therefore little dissipation. There is always a compromise that must be taken. (20)

2.5.3 Static equilibrium

For the characterization of the mechanical properties of textile reinforcements the static relaxation behavior can be analyzed. This is perceived when a test sample is subject to a deformation which is kept constant for a defined time. In this case, the test body experiences a spontaneous increase in stress, which decreases during the hold time until the equilibrium is reached. Figure 5 schematically shows the strain and stress curve. (22)

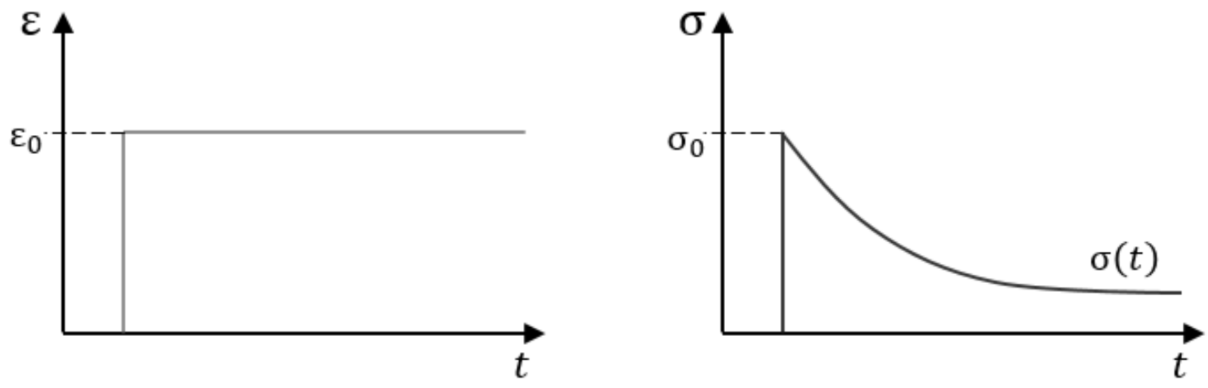

Figure 5 – Elongation-stress ratio during relaxation (22)

2.5.4 Dynamic Mechanical Analysis

DMA is a technique that uses dynamic perturbations to study the response of materials to stress, temperature, frequency and other parameters.

In order to characterize the viscoelastic behavior of a material, the material is sinusoidally deformed, and the resulting stress is recorded. Figure 3 shows a viscoelastic response with a phase lag between the stress and the strain. (22) (4)

The material is subjected to an oscillatory strain with frequency ω. The following expressions describe strain and stress: (22) (4)

$$\varepsilon = \varepsilon_0 \sin(\omega t) \tag{3}$$

$$\sigma = \sigma_0 \sin(\omega t + \delta) \tag{4}$$

In Equation 4, δ is the phase lag between the stress and strain. From these expressions, two moduli are defined: (22) (4)

$$E' = \left(\frac{\sigma_0}{\varepsilon_0}\right) \cos\delta \tag{5}$$

$$E'' = \left(\frac{\sigma_0}{\varepsilon_0}\right) \sin\delta \tag{6}$$

E' is known as the storage modulus and E'' as the loss modulus. Alternatively, using complex variables: (22) (4)

$$\varepsilon = \varepsilon_0 \exp i\,(\omega t) \tag{7}$$

$$\sigma = \sigma_0 \exp i\,(\omega t + \delta) \tag{8}$$

$$E = \frac{\sigma}{\varepsilon} = \left(\frac{\sigma_0}{\varepsilon_0}\right) \exp i\,\delta = \left(\frac{\sigma_0}{\varepsilon_0}\right) (\cos\delta + i\sin\delta) = E' + iE'' \tag{9}$$

Figure 6 shows the graphical relationship between these variables. The storage modulus is a measure of the stored energy, i.e., the elastic part, while the loss modulus is a measure of the energy lost as heat, i.e., the viscous part. (22) (4)

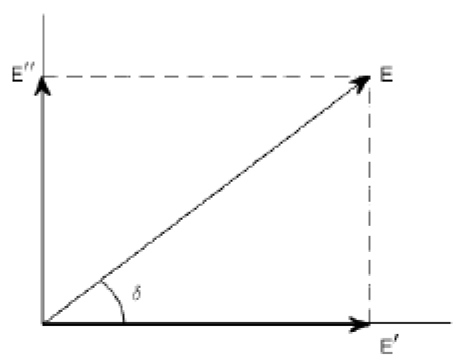

Figure 6 - Vectorial representation of the complex modulus. (22)

A new term called the loss factor can now be defined as follows:

$$\text{Loss factor} = \tan\delta = \frac{E''}{E'} \tag{10}$$

This term is proportional to the ratio of the maximum energy dissipated per cycle to the maximum energy stored in the cycle. (22) (4)

The evaluation of these variables is important to describe the viscoelastic and hysteresis behavior of the reinforcement materials analyzed in this thesis. (4)

3 Materials and Methods

3.1 Stepwise relaxation test and basic procedure

Zwick / Roell testing machine was used for testing under static conditions. This machine is electrically driven with traverse that is guided over a running rail or steel column. The recording of the parameters is performed by measuring systems, which are connected to a computing unit and make available the possibility to set various test specifications. The basic structure is shown in Figure 7.

Figure 7 - Zwick / Roell static testing machine (13)

Various parameters such as force, displacement and strain can be measured. To ensure a temperature-controlled test setting, there is a climate chamber around the terminal structure. This offers the possibility to regulate the temperature with a homogeneous distribution in the chamber. A range of temperature from -80 to 250 °C can be set with an accuracy of ±0.5 °C. The cooling is via the supply of nitrogen. Further technical data of the climate chamber is shown in Table 2.

Table 2 – Climate chamber specifications

Temperature range / °C	-80 to 250
Temperature regulation accuracy / °C	± 1
Heating rate / K min	Until 12
Cooling rate / K min	Until 5,5
Test dimensions / mm	700 x 260 x 460

The tensile test is an important method for the study of materials and it makes possible the evaluation of the temperature dependency at fully relaxed state.

For the evaluation of the thermodynamic equilibrium behavior, this test method replicates the equilibrium state during slow loading processes. Thus, the viscoelastic behavior of the textile reinforcements can be described at a specific temperature. Assuming that the cords relax around the viscous stress component after waiting for constant elongation, the elongation of a cord sample should be gradually increased. Here, the holding time should be chosen so that the cord approaches the state of equilibrium avoiding a long running test time. With this approach, the time-dependent viscous component caused by the relaxation should decrease over time and point to the equilibrium status.

In this study, three different materials were evaluated. Nylon, hybrid and polyester were the textiles tested at different isothermal conditions at 23, 40, 80, 110 and 160 °C. These tested materials were submitted to tensile stress. The stress-strain curve response of the tested materials at different temperatures allows an evaluation of the tested material´s characteristics.

Before starting the test procedure, the defined temperature in the climatic chamber must be reached. After reaching the selected temperature, the waiting period before clamping the sample was of 60 min. Pneumatic clamping was used for the static tests. After the temperature was reached and the waiting time ensured, the sample was clamped before the start of the test and the force applied to the cords was established to be lower than the pre-load applied for the specific material construction.

The required preload for each textile cord was calculated as shown in Equation 13. Hybrid cords were of Nylon 1400x1 and Aramid 1670x1 yarns twisted together. The required pre-load was calculated from the individual yarns and added afterwards.

$$Preload = linear\ density\ \cdot 0{,}005\ \cdot\ number\ of\ yarns \tag{11}$$

The calculated preliminary forces for the textile reinforcements used were grouped as shown in Table 3, including the strain rates managed for testing each material. The specimens have been obtained from production and were in the form of a spool or as a fabric, as specified in Table 3 where are grouped in some conditions of the test trials.

Table 3 – Static test specification

Material	Nylon	Polyester	Hybrid
Construction	470x2	1440x2	Aramid 1680 + Nylon 1400
Samples taken from	Spool	Fabric	Spool
Preload / N	0,47	1,44	1,54
Strain rate / mm min^{-1}	120	120	120
Temperature / °C	23, 40, 80, 110, 160		
Relaxation strain range / %	2,5 to 15	2,5 to 12,5	2 to 10
Relaxation strain incrementation steps / %	2,5	2,5	2
Holding time / min	10		
Clamping pressure / bar	6	6	4
Gauge length / mm	250		

After the sample has been taken in the experimental set-up, it was loaded with the specific pre-load within 60 s and kept constant for 5 min. This step was required to achieve a homogeneous temperature distribution in the chamber, since the heat can escape when opening the chamber for the clamping of the sample. After the previously referred waiting time, the sample was loaded in order to achieve the first deformation stage ε_1 and then hold for 10 min to accomplish fully relaxed samples. This step was repeated until the last strain level was achieved. The stress-strain plot, shown in Figure 8, represents the procedure used for the stepwise relaxation tests.

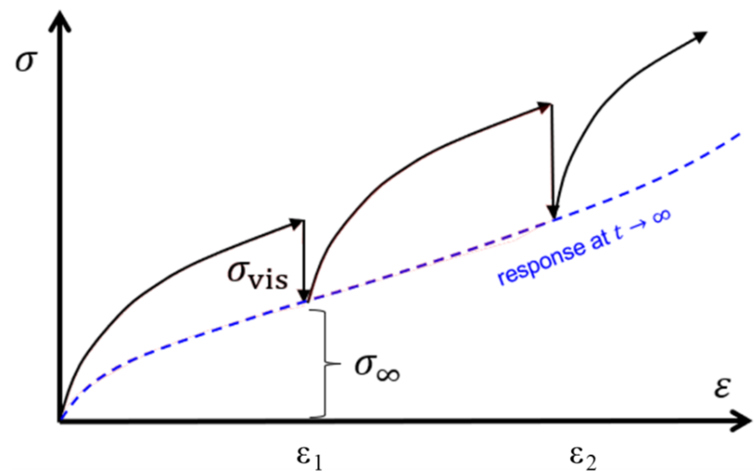

Figure 8 – Stress distribution for stepwise relaxation experiment and estimated equilibrium stress

In Figure 8, the variables ε_1 and ε_2 represent the first two strain relaxation steps, which are specified in Table 3 for each material tested. The blue slashed curve exemplifies a specific material at the fully relaxed state and was acquired by combining each final value of all strain relaxation steps analyzed.

First, for each test condition five to four samples were used per each defined temperature. Meanwhile it was observed that three and even two samples per temperature were enough to characterize the curve behavior.

3.2 Dynamic test system and basic procedure

3.2.1 Characterization of the dynamic test

MTS Acumen 3 Test System, represented in Figure 9, connected to a MTS Flextest 40 Controller and the Multipurpose Testware (MPT) and Elite (MPE) applications were used to perform the dynamic tests with a Mytron KPK 27 KH Climate Chamber for temperature and humidity control. This configuration allows the creation and operation of an automated and customized test procedure, as well as the acquiring of the data throughout the test. (4)

Figure 9 – MTS Acumen 3 testing machine (13)

Various parameters such as E‘, E‘‘ and tan δ could be calculated following DIN Specification 53513. (23)

To ensure a temperature-controlled test setting, the climate test cabinets of the KPK KH series was used. A range of temperature from -70 to 180 °C could be set with an accuracy of ±0.5 °C. Some specifications are shown in Table 4.

Table 4 - Mytron KPK 27 KH climate chamber specifications (24)

Temperature range / °C	-70 to 180
Temperature regulation accuracy / °C	± 0,5
Humidity range / %	10 to 96
Humidity constancy /%	± 2,5
Cooling	Water-cooled
Power consumption / kVA	1 to 5
Test dimensions / mm	420 x 480 x 320

The parameters temperature and relative humidity were controlled by compact controllers. (24) The design of Flextest controllers was based on decades of MTS expertise in providing solutions for structural, system, component and material testing.

In this phase of the work PET and Nylon 6.6 were tested. All samples meant to be tested were previously stored in a controlled environment at 23 °C and 55% humidity. Before the start of the test procedure the defined temperature of 23 °C in the climatic chamber was achieved. After reaching the selected temperature, the waiting period following the pneumatic clamp of the sample was of 60 min. After the desired temperature was reached and the waiting time ensured, the sample was clamped, and the force applied to the cords was established to be lower than the pre-load applied for the specific material construction. The required preload for each textile cord was calculated as shown before in Equation 13. Then, the displacement was offset to guarantee that the samples were standardized.

After that two phases took place before the desired dynamic test begun – pre-condition and pre-deformation represented in Figure 10, respectively as number 1 and 2. Pre-condition consisted of 10 cycle loads with magnitude of 1 to 8%, responsible to condition the cord sample. Then a desired strain level was reached, and it was hold for 5min to allow the fully relaxation of the cord material; being this the stated pre-deformation. The last stage consisted on oscillating strain with defined strain amplitude at specific temperatures and frequencies specific for each test procedure and is represented as number 3 in Figure 10. The following steps comprised the test procedures described in Subsections 3.2.2 to 3.2.5.

For a better insight, the conditioning procedures are showed in Figure 10.

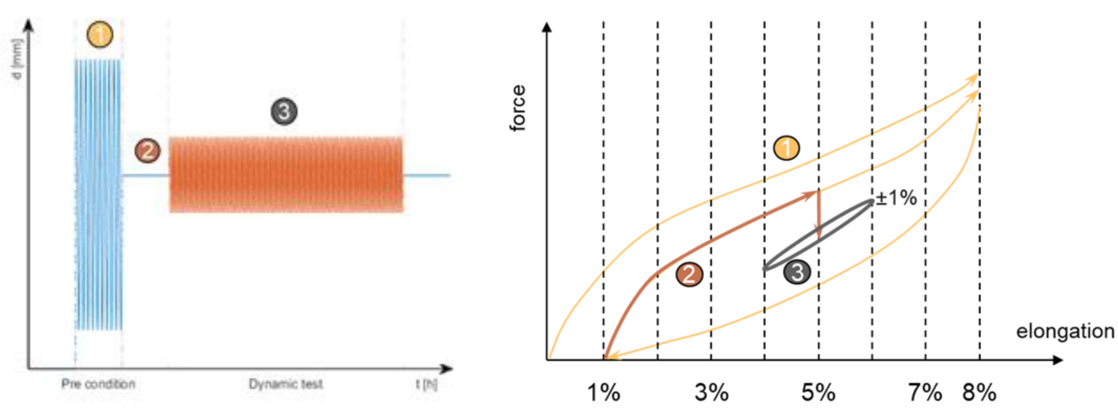

(a) (b)

Figure 10 – Illustration of the general dynamic test procedure displayed in two configurations: a) displacement-time b) force-elongation

Cords can experience buckling when dynamically tested due to limitations of the MTS machine. In pre-conditioning stage, the cord is expected to elongate. Due to MTS machine restraints, when the cord is stretched into the desired pre-deformation this strain previously defined may not correspond to the real strain value that the cord samples is experiencing while being tested. In fact, MTS machine assumes the reference length as the initial length of the sample and, due to that, even though the cord may experience elongation throughout the test, the MTS machine do not change this reference length. As the stain level is related to the length of the cord, which may have an inaccuracy because of possible increase of length at the pre-conditioning stage, the real length can be lower than the defined in the test procedure. This way, even though it is not expected, some strain amplitudes of the oscillating stress applied might be too high for the cord, which leads to buckling.

With dynamic tests it was possible to study the influence of parameters that affect the mechanical properties of textile reinforcement cords such as frequency, temperature, static pre-deformation and strain amplitude.

3.2.2 Effect of temperature at a wide range of frequency

Frequency and temperature affect the mechanical and thermomechanical properties of textiles. These two parameters can be related based on the Time-Temperature Superposition (TTS) principle.

A wider range of frequency than the reachable by direct measurements can be obtained via this TTS principle and its application is illustrated in Figure 11. This principle was used for the construction of the master curves that describe the mechanical properties of PET over frequency at a specific temperature.

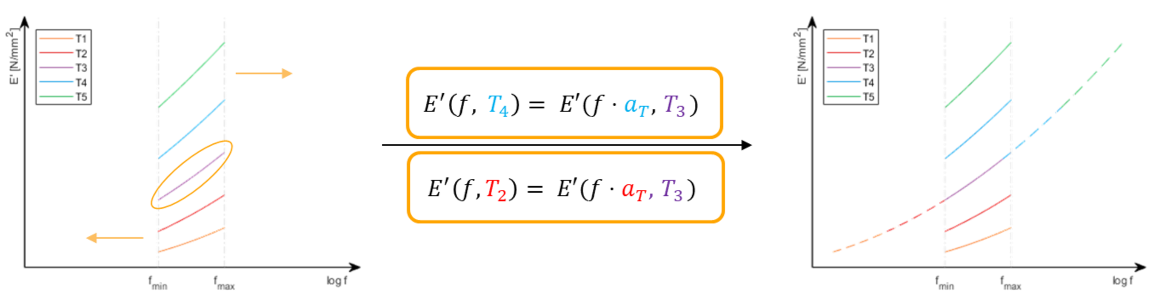

Figure 11 - Illustration of the master curve construction

Lower temperatures were shifted manually to higher frequencies, and vice-versa, to get a smooth curve as shown in Figure 11 represented as a dashed curve. This shifting of the isothermal frequency sweeps curves to a reference temperature was used to create the master curve at a reference temperature.

For that, dynamic tests were performed for PET 1440x2 at different frequencies and temperatures and some specifications are showed in Table 5.

Table 5 – Master curve test specification

Material	Polyester
Construction	1440x2
Samples taken from	Fabric
Preload / N	1,44
Strain rate / mm min^{-1}	120
Temperature / °C	-20 to 180
Temperature incrementation steps / °C	20
Frequency / Hz	1 to 30
Clamping pressure / bar	6
Gauge length / mm	100

These tests involved decrease of frequency sweeps nested in increase of temperature sweeps. Frequencies were selected from 1 to 30 Hz in a logarithmic equal scale distribution and temperatures from -20 to 160°C with an increment of 20 °C, as shown in Table 5 and Figure 12.

Starting with the highest frequency of 30 Hz conditions the following blocks of frequencies, which mean that the convergence rate is higher for these blocks. This conditioning leads to a decrease of the testing time. Higher frequencies than 30 Hz would cause mechanical resonance, affecting the monitored test data. The lowest frequency used was 1 Hz due to the load cell's resolution capacity. Lower frequencies would cause significant noise of the transducer. (4)

The frequency of 30Hz had a dwell period of 2h, which conditioned the lower frequencies, having each a dwell period of 20 min. The frequency conditioning of the lower frequencies decreased their time of stabilization.

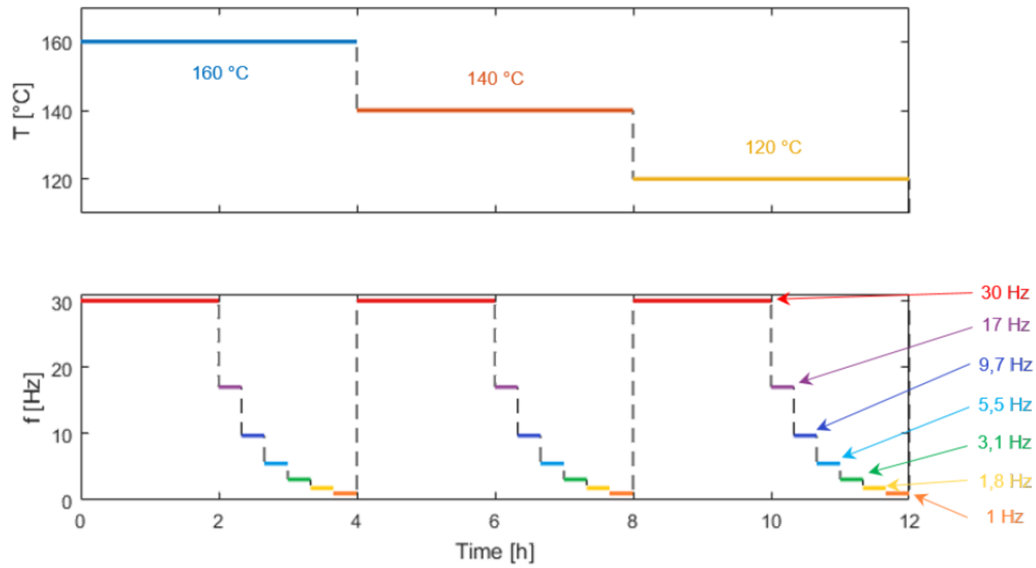

Figure 12 - Representation of the nested frequency sweeps in a temperature sweep procedure, with decreasing temperature steps. (4)

For each condition of temperature and frequency, it was predicted the limit value of E', E'' and tan δ with an asymptotic regression, using the function shown in Equation 14 in MATLAB.

$$y = \theta_1 - \theta_2 \exp(-\theta_3 \times t) \tag{12}$$

$$\lim_{t \to \infty} y = \theta_1 \tag{13}$$

An example of the function fit as is shown in Figure 13 and the steady state value to time infinite is represented by θ_1 and shown in Equation 15.

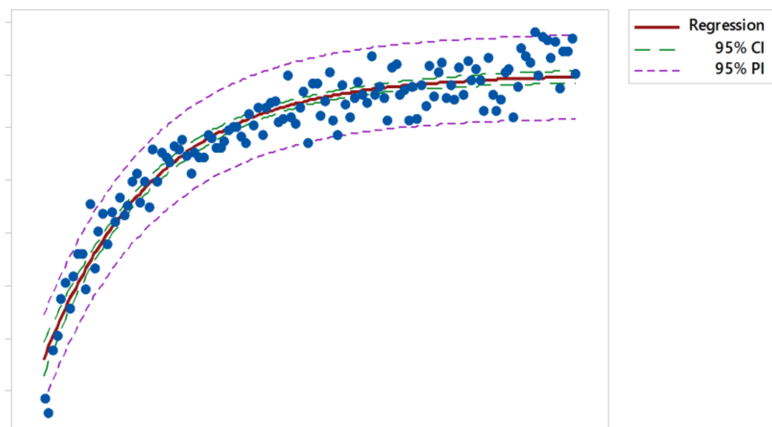

Figure 13 – Example of a nonlinear regression fit of data

All data results of frequencies and temperature combinations need to reach stability in order to assume that the testing time is adequate and that the predicted limit values for all modulus are accurate.

Based on this procedure, the frequency and temperature dependence of the dynamic material properties were analyzed. Furthermore, the temperature frequency shifting technique can be applied to establish the master curve.

For this procedure 3 samples have been tested in the same conditions to guarantee the evaluation of the of the results variability. For analysis purposes the sample curve that was closer to the mean values of all tested samples was chosen to stand for the data settings procedure as described in Subsection 4.2.

3.2.3 Effect of static pre-deformation at a wide range of frequency

The static pre-deformation of the dynamic tests described so far were performed with 6% of static pre-deformation. To evaluate the effect of the pre-deformation on the mechanical behaviour of PET, different pre-deformation was tested and the cord response was analysed. In Table 6 are grouped in some conditions of the experiments.

Table 6 - Static pre-deformation specifications

Material	Polyester
Construction	1440x2
Samples taken from	Fabric
Preload / N	1,44
Strain rate / mm min^{-1}	120
Temperature / °C	23
Strain / %	5 to 8
Strain incrementation steps / %	1
Strain amplitude / %	±1
Clamping pressure / bar	6
Gauge length / mm	100

The test procedure consisted of frequency sweeps nested in pre-deformation sweeps. Four different pre-deformation from 5 to 8% were tested at 23 °C and fixed strain amplitude of ±1%. Figure 14 shows the displacement evolutions of the test procedures.

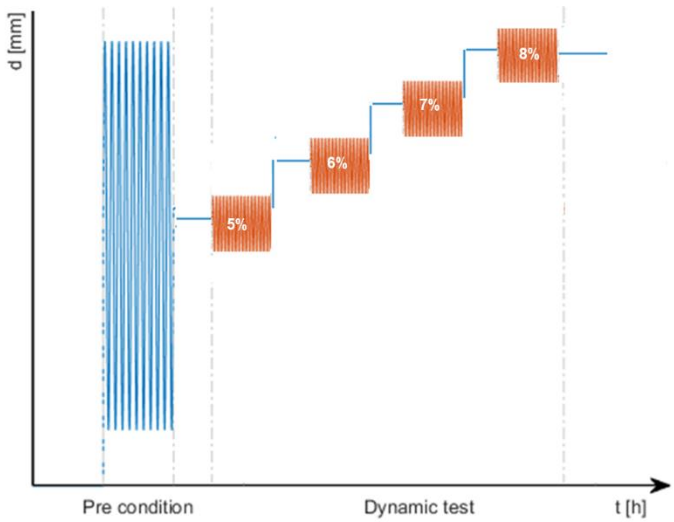

Figure 14 – Illustration of the static pre-deformation test procedure

In each strain amplitude sweep of this dynamic test, there were nested frequencies sweeps from 1 to 30 Hz. The first frequency of each strain amplitude sweep is 30 Hz, lasting 1 h, and the following frequencies sweeps lasted each 20 min. This frequency testing was the same used in all the described procedures of Subsections 3.2.2 to 3.2.4.

For this procedure 3 samples have been tested in the same conditions to evaluate the variability of the results. For analysis purposes the sample curve that was closer to the mean values of all tested samples was chosen to represent the data settings procedure and was evaluated in Subsection 4.3.

3.2.4 Effect of strain amplitude at a wide range of frequency

The strain amplitude effect on the mechanical properties of textile cords was evaluated under dynamic conditions. In this stage the same material construction PET 1440x2 was tested with different strain amplitudes. In Table 7 are grouped some specifications of the experiments.

Table 7 - Strain amplitude test specification

Material	Polyester
Construction	1440x2
Samples taken from	Fabric
Preload / N	1,44
Strain rate / mm min^{-1}	120
Temperature / °C	23
Strain / %	6
Strain amplitude / %	±0,5 to ±2
Strain amplitude incrementation steps / %	0.5
Clamping pressure / bar	6
Gauge length / mm	100

The test procedure consisted of frequency sweeps nested in strain amplitude sweeps. Four different strain amplitudes from ±0.5 to ±2% were tested at 23 °C at a fixed pre-deformation of 6%. Figure 15 represents the displacement evolution of these test procedure.

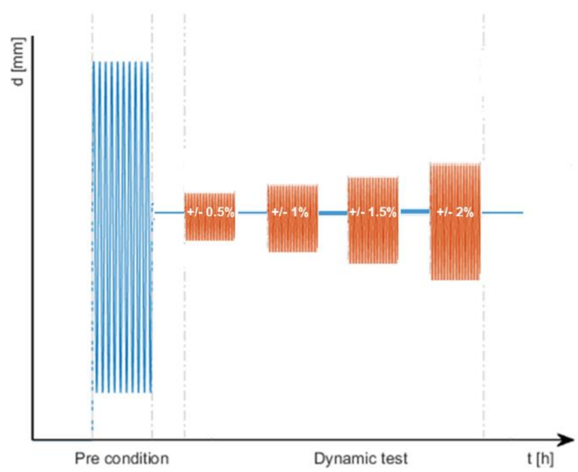

Figure 15 – Illustration of the strain amplitude test procedure

Figure 15 show pre-condition and pre-deformation stages and the strain amplitudes sweeps at a fixed pre-deformation of 6%.

For this procedure 3 samples have been tested in the same conditions for evaluation of the variability of the results. For analysis purposes the sample curve that was closer to the mean values of all tested samples was chosen to represent the data settings procedure and was evaluated in Subsection 4.4.

3.2.5 Temperature monitoring of textile cords

PET cords seem to take longer time than Nylon 6.6 to reach steady state when holding cyclic loading. (4)

Thus, PET and Nylon 6.6 with different linear densities were tested, focusing on the variation of their cords' temperature under dynamic conditions. In Table 8 it is shown some specifications of the experiments.

Table 8 - Temperature test study specification

Material	Polyester	Nylon
Strain rate / mm min^{-1}	120	
Temperature / °C	Room temperature	
Strain / %	6	
Strain amplitude / %	±1	
Frequency / Hz	10	
Clamping pressure / bar	6	
Gauge length / mm	100	

At room temperature, PET and Nylon 6.6 were dynamically tested with 6% of static pre-deformation and strain amplitude of ±1. Each material had two extreme linear densities with the closest twist factor available at that time. The cord specifications are shown in Table 9.

Table 9 – Cords specifications of temperature test study

Material	Nylon		Polyester	
Construction	940x2	2800x2	630x2	2200x2
Samples taken from	Spool	Fabric	Fabric	Fabric
Preload / N	0,47	2,80	1,44	2,20
Twist factor	151,76	194,57	191,68	199,00

Unlike the previous tests, the temperature measurements were not of the chamber but of the textile cords. Doing so allowed the tracking of temperature evolution throughout the test. An infrared thermal camera was used to capture thermal images during tests.

An Infrared Thermal Camera Fluke Ti25 IR Fusion Technology was used to take thermal photos for temperature validation of the temperature measurements trend response of the cords performed by the MTS machine.

In addition, the material construction of PET 1440x2 described in Subsections 3.1 to 3.2.4 were tested at RT and 10Hz at the same 6 % of pre-deformation and ±1 % of strain amplitude for 60h to detect the material response throughout the test. For this procedure 3 samples have been tested per each different material construction to evaluate the variability of the results.

Additionally, a single sample test for PET 2200x2 was performed with the same procedure at 30 Hz.

4 Results and Discussion

This chapter is divided into five parts that correspond respectively to the Subsections 3.1 and 3.2.2 to 3.2.5.

4.1 Effect of temperature at fully relaxed state

These tests consist on increase of force to reach specific strain levels of the material tested followed by relaxation as described in more detail in Subsection 3.1.

The mean force values of the polyester testing samples for each temperature were plotted and are shown in Figure 16.

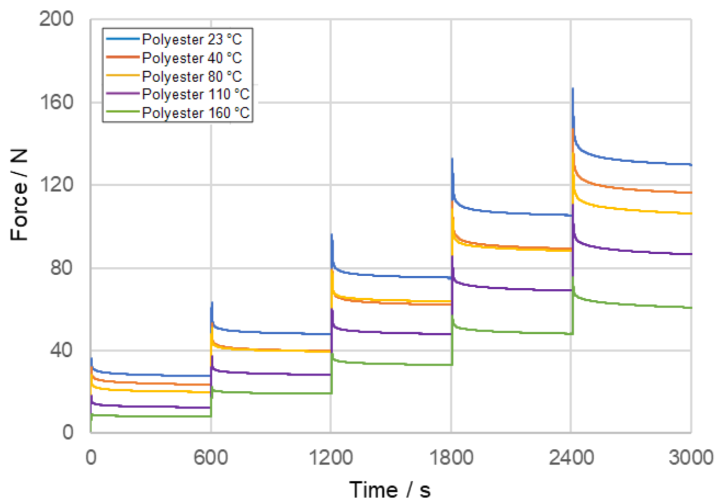

Figure 16 – Representation of the mean force versus time at different temperatures for polyester

It seems that the force stabilized in all breakpoints: 600, 1200, 1800, 2400 and 3000 s. This suggests that the hold time of 10 min is enough for polyester to readjust to the relaxed state.

For analysis purposes, the thermodynamic equilibrium is shown in a stress-strain plot (Figure 17).

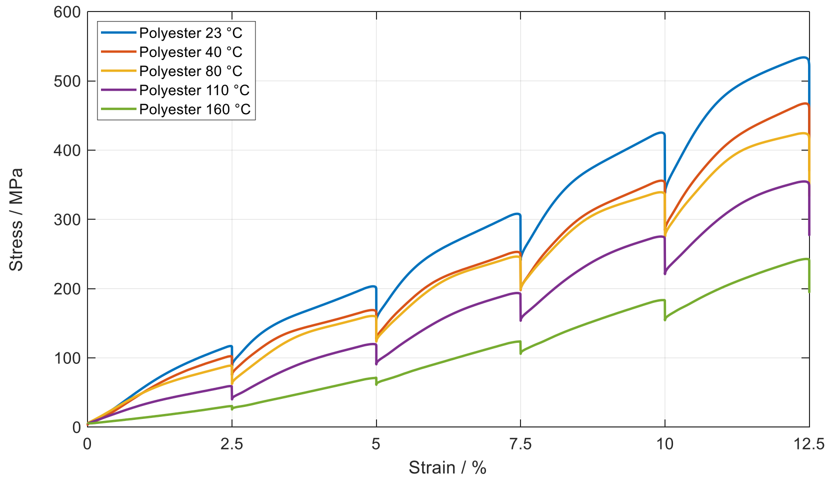

Figure 17 - Stress distribution for stepwise relaxation experiment

Figure 17 shows the relaxation behavior of polyester 1440x2 at the temperatures presented in Table 10. One can see that a decrease in stiffness goes together with the increase in temperature possibly due to the shift of molecular chains dependency on temperature.

Table 10 - Stress variation in each relaxation strain steps at different temperatures for PET 1440x2.

Δ Stress / MPa		ε / %				
		2,5	5	7,5	10	12,5
Temperature / °C	23	27,4	49,1	65,6	85,0	117,2
	40	26,4	41,8	54,1	70,0	97,8
	80	25,2	36,7	46,8	62,0	89,9
	110	18,0	29,2	39,4	52,9	77,3
	160	5,01	10,2	17,9	29,1	48,0

A curve that passes by all breakpoints is the prediction of the thermal equilibrium curves of PET cords at a specified temperature and is represented in Figure 18 by dashed curves.

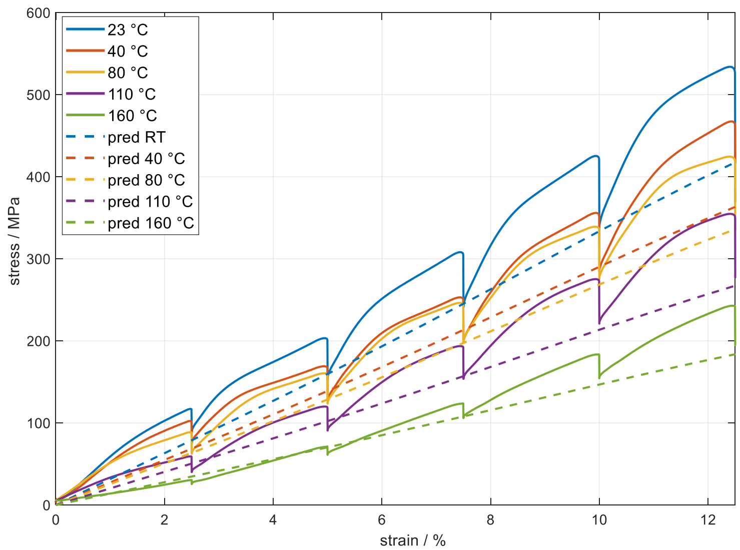

Figure 18 - Stress distribution for stepwise relaxation experiment and estimated equilibrium stress for PET 1440x2

Figure 18 displays the thermal equilibrium curves for 23, 40, 80, 110 and 160 $°C$. Stress increases with increasing strain as expected due to higher force needed to achieve higher strain levels. The slope of the estimated equilibrium stress curves represented with dashed lines decrease at higher temperatures which seems to suggest that stiffness decreases with increase of temperature.

Estimated equilibrium stress curves of 40 and 80 °C almost overlap. The stiffness of polyester seems to be similar for both temperatures which suggest that the material properties are similar. This can be explained due to the PET thermal polymer´s transitions. In the next chapter this behavior will be further addressed.

For curves other than 40 and 80 °C, temperature seems to contribute to a greater impact on the material response behavior and a shifting in the stress axis was observed.

To check if these material properties are the characteristic behavior of textile reinforcement cords or specific to PET 1440x2 other textiles were tested - hybrid and nylon.

The stress-strain plots for all tested samples for nylon, hybrid and polyester are presented in Appendix B.1. Figure 19 shows the results of the measurements for the hybrid and nylon textile reinforcements.

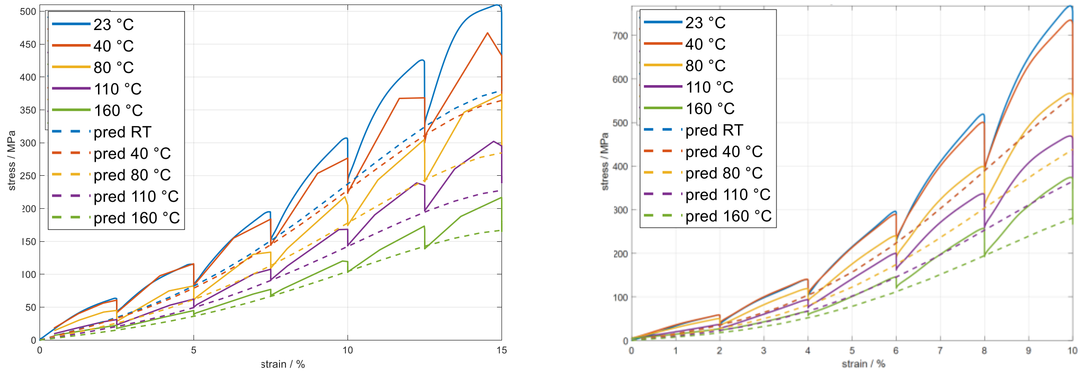

(a) (b)

Figure 19 – Stress-strain curves for different temperatures in the relaxation test for different materials: a) Nylon 470x2 b) Hybrid 1680 +1400

For these material constructions the holding time seem to be enough to reach the full relaxed state and their force-time plot are shown in Appendix B.1.

As with polyester, the nylon cords display similar behavior response at 23 and 40 °C. However, for hybrid cords the material show similar response properties at 40 and 80 °C. Each polymer seems to have a specific thermal transition, and this is likely to be the reason for the differences in their thermal-mechanical properties. Figure 19 also shows that for all materials the overstress decreases at elevated temperature, which seems to imply that the hysteresis properties have dependence on temperature. For a better understanding of this phenomenon, the temperature effect on hysteresis properties for PET 1440x2 is described in Subsection 4.2.

4.2 Effect of temperature at a wide range of frequency

As described in Subsection 3.2.2, experiments with different frequencies and temperatures were performed. For the analysis of the convergence at each condition the storage modulus was plotted over time and the results are shown in Figure 20. Results of E’’ and tan δ over time are available in Appendix B.2.

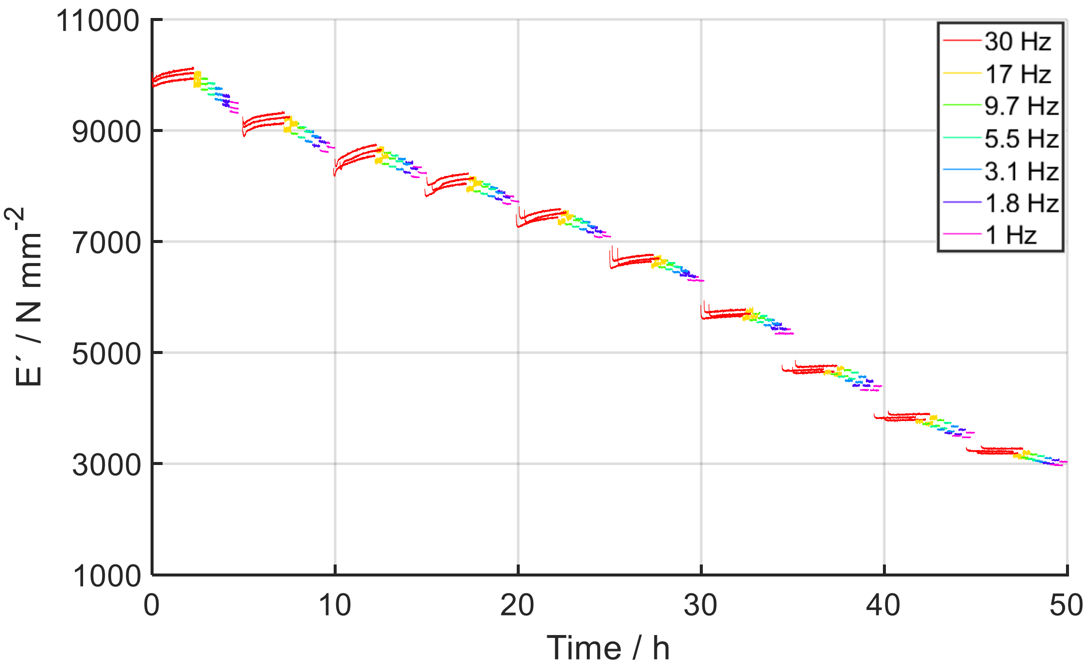

Figure 20 –E' over time from the nested frequency sweeps in a temperature sweep procedure for three samples.

It seems that the frequencies at all temperatures reached steady state for all the 3 samples tested. This means that 2 h seems to be enough for the curves to converge to equilibrium for their specific frequency and temperature combination. Furthermore, all three samples show an inconsistency between samples that seems to be restrained in sample variation. These acceptable deviations between samples at the same condition occurred in all the tests presented in this work.

For each combination of frequency and temperature the limit values were predicted with the fitting procedure explained in Subsection 3.2.2. The values of this curve are represented over frequency in Figure 21 and over temperature in Figure 22. These data results for all samples are presented in Appendix B.2.

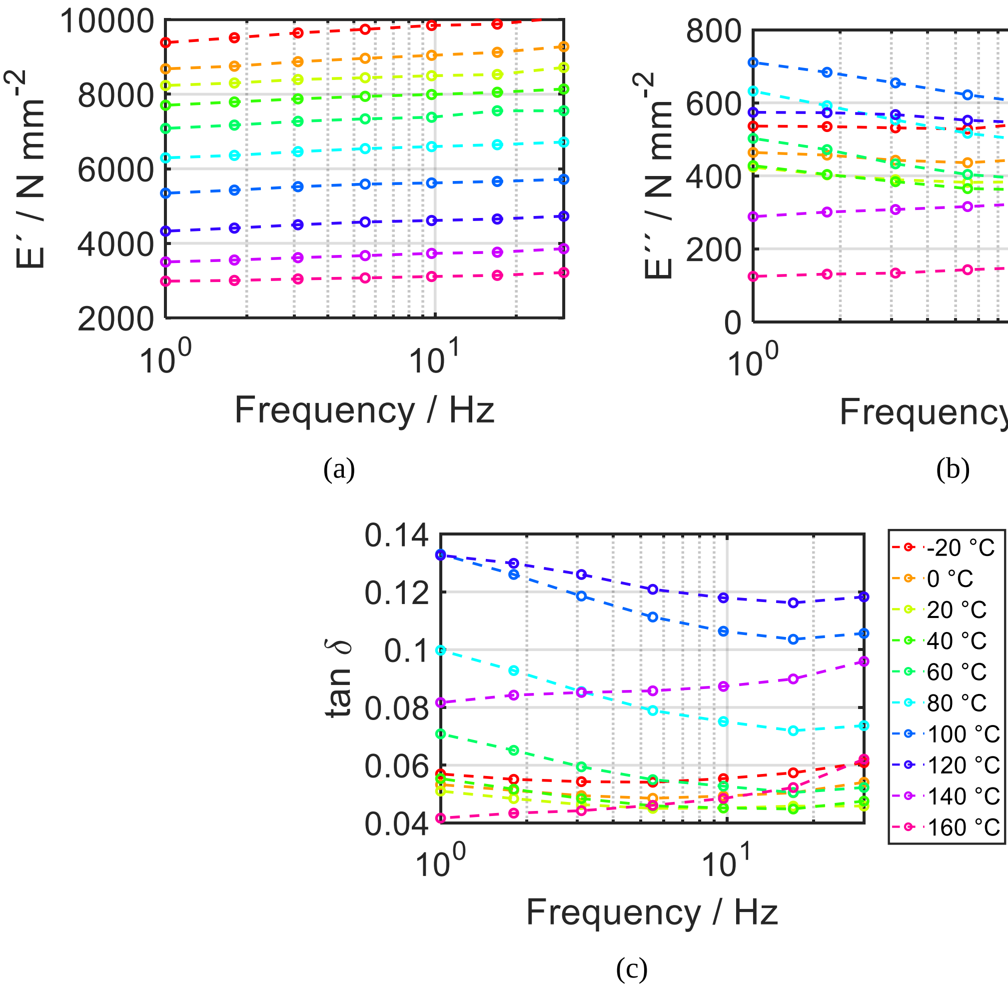

Figure 21 – Modulus predicted values over frequency at different temperatures a) E' b) E'' c) tan δ

E' decreased with increase of temperature. The increasing softening of the material with temperature seems to explain this behavior and fits with the results of Subsection 4.1. Likewise, all modulus displayed almost a linear curve behavior with increasing of frequency except for 30Hz. For all samples the values of 30 Hz did not always follow the curves trend and because of that were not used for the construction of the master curve. The reason of this unexpected behavior might be resonance on the MTS machine related to the frequency of 30 Hz.

Figure 21 shows that the dependency of E'' and tan δ on temperature do not seem to correlate. However, the modulus representations over temperature provide a better perception about the mechanical properties of PET 1440x2.

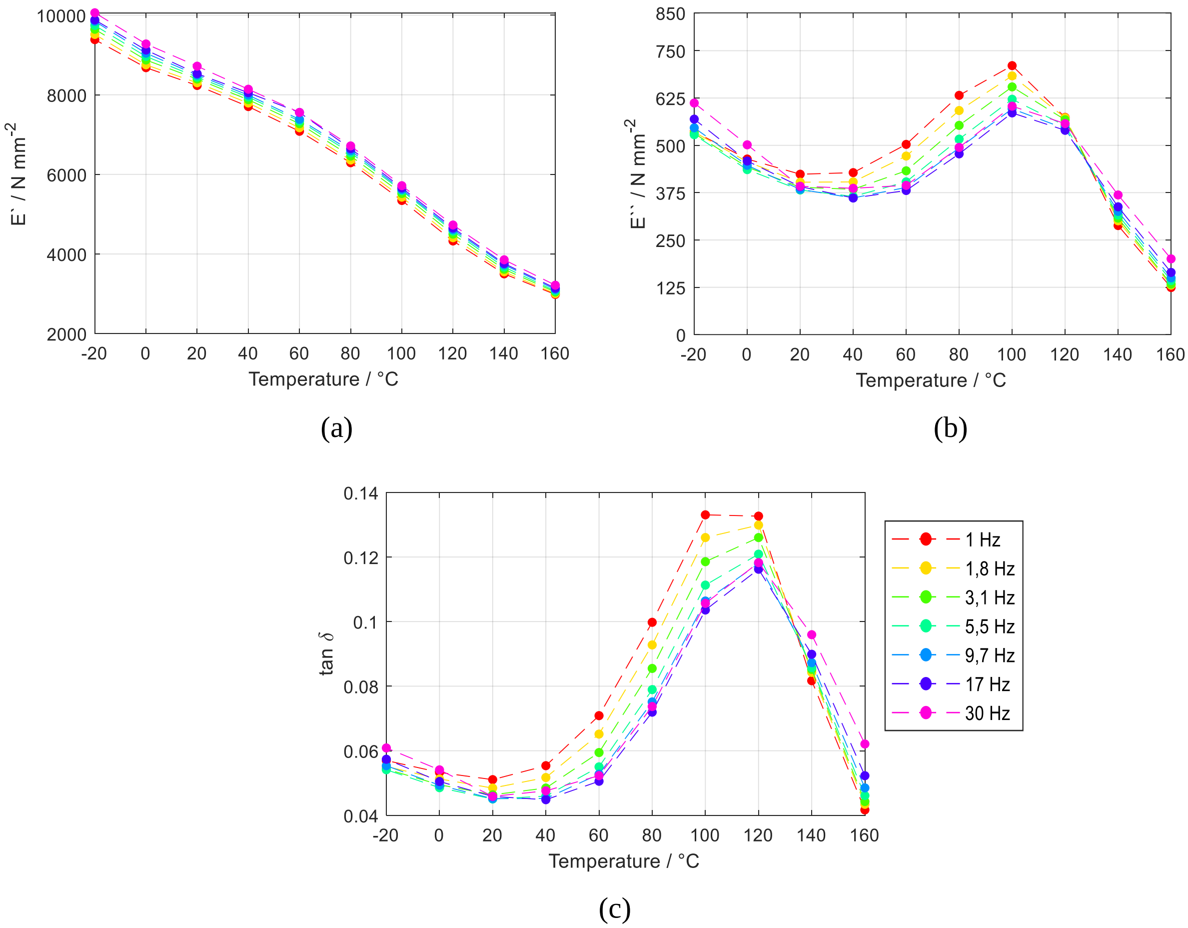

Figure 22 - Modulus predicted values over temperature at different frequencies a) E' b) E'' c) tan δ

In addition, in the studied temperature range, two changes in E' slope are observed, from 40 to around 80 °C, and from 100 to 140 °C. These changes go together with a peak in E'', between 80 and 120 °C and in tan δ, respectively, between 80 and 140 °C.

These variations can be explained by thermal transitions in the polymer, indicating how the molecular motions and free volume changes affect its behavior. (25) In fact, similar values have been described in the literature, consistent with the glass transition. While the reported transition ranges are close to the detected ones, minor differences might be explained by additional factors, such as differences in the level of crystallinity. (4)

4.3 Effect of static pre-deformation at a wide range of frequency

As described in Subsection 3.2.3, experiments with different pre-deformation were performed at a strain amplitude of ±1% for different frequencies and temperatures. For the analysis of the convergence at each condition, the storage modulus was plotted over time and the results are shown in Figure 23. Results of E'' and tan δ over time are presented in Appendix B.3.

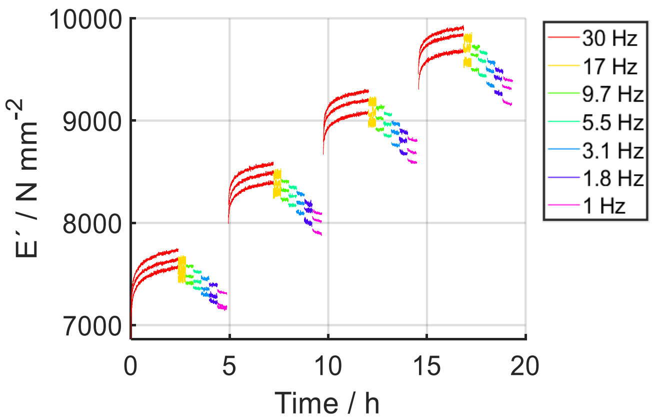

Figure 23 - E' over time from the nested frequency sweeps in pre-deformation sweeps for three samples.

Since all frequencies and temperature combination reached stability for all the 3 samples tested, it was assumed that the testing time was adequate for each sample.

The fitted prediction values of the data taken from testing are showed in Figure 24. The same results for all samples are presented in Appendix B.3.

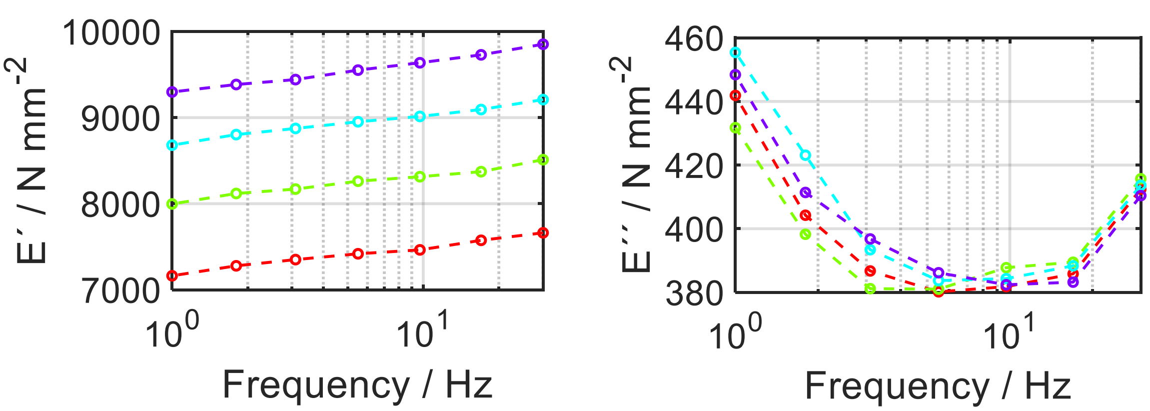

(a) (b)

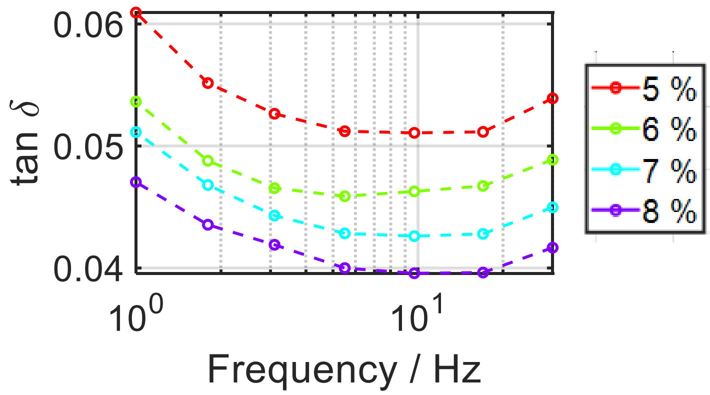

(c)

Figure 24 - Modulus predicted values over frequency at different pre-deformations a) E' b) E'' c) tan δ

E' increased with increase of pre-deformation due to material stiffening with increase of pre-deformation, which fits with the response of rubber reported in the literature (26). E' seems to have a linear curve behavior with increase of frequency. E'' and tan δ seem to have a curvature pattern behavior with increase of frequency. However, the values of E'' did not seem to change much for different pre-deformations. This was clear even at 1 Hz were the highest value change occurred, as shown in Figure 25.

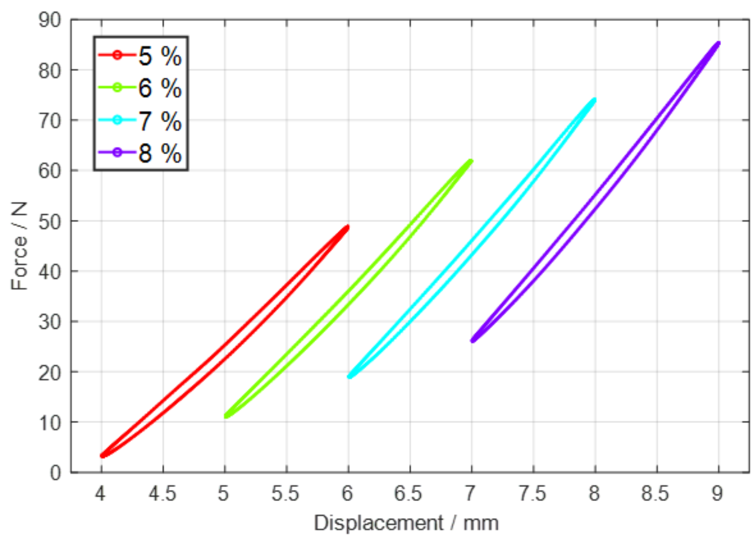

Figure 25 - Hysteresis last cycle for each pre-deformation

As shown in Figure 25 the amount of hysteresis, given by the area, seems to be similar, which means that E'' does not appear to change substantially within the range of pre-deformation selected for this test.

Noteworthy, at least one of the combinations of the test herein described and the one described in Subsection 4.2 share the same experiment conditions. The comparison between both pre-deformation and temperature tests is shown in Figure 26.

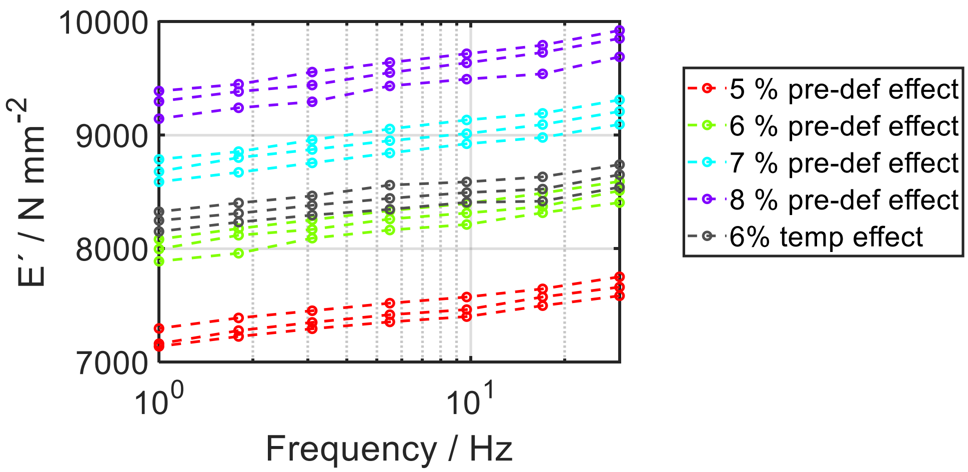

Figure 26 - E' over frequency at different pre-deformations comparison with Subsection 4.2.

Interestingly, the values of E` almost overlap for both tests which may indicate that the material responds similarly when submitted to the same conditions. This is an outcome that may be useful for the validation of the reliability of the procedures in this study: different procedure methods lead to similar results in the mechanical behavior of the tested material. Actually, it seems to be a good indicator of the accuracy of the data results herein reported. Worth mentioning, both tests conditions share a difference in temperature of 3 °C, which does not seem to be substantial for the material properties to change.

4.4 Effect of strain amplitude at a wide range of frequency

As described in Subsection 3.2.4, experiments with different strain amplitudes were performed at a specific pre-deformation of 6% for different frequencies and temperatures. For the analysis of the convergence at each condition, the storage modulus was plotted over time and the results are shown in Figure 27. Results of E'' and tan δ over time are reported in Appendix B.4.

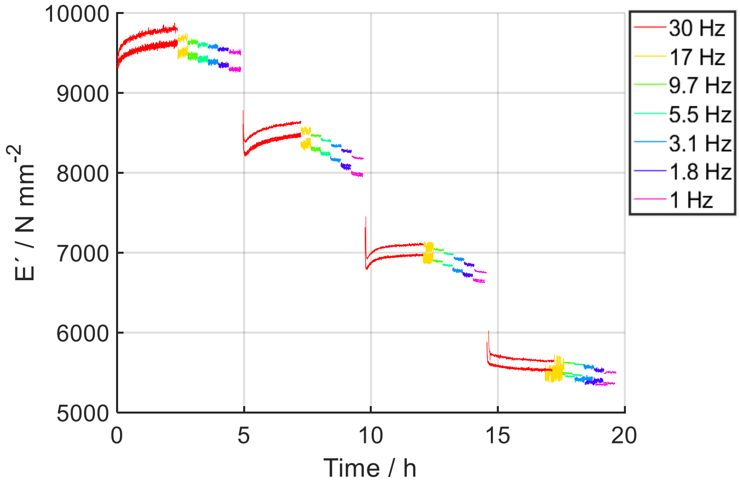

Figure 27 - Results of E’ over time from the nested frequency sweeps in a strain amplitude sweep procedure for three samples.

All frequencies and temperature combinations reached stability for all the 3 samples tested, thus, it seems that the testing time was adequate for each condition.

The fitting prediction values of the data results taken are represented over strain amplitude in Figure 28. The results for all samples are reported in Appendix B.4.

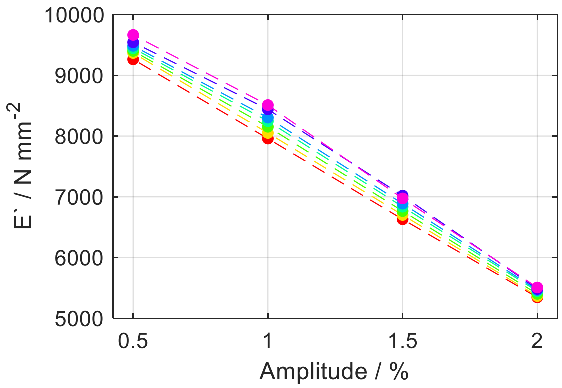

(a)

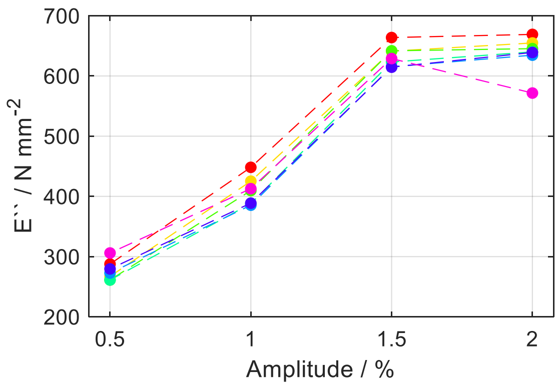

(b)

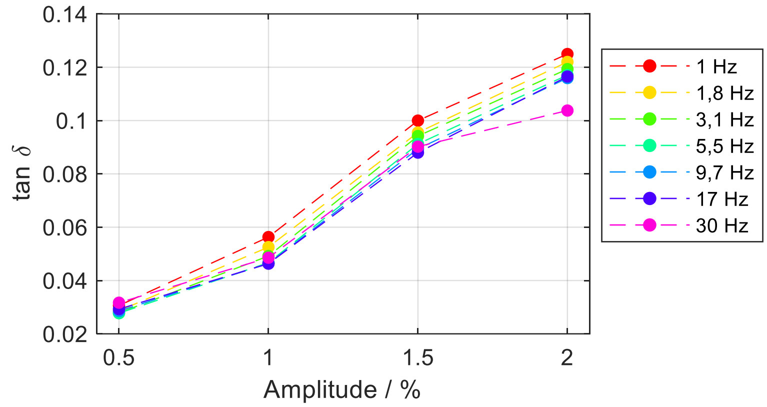

(c)

Figure 28 – Modulus predicted values over strain amplitude for different frequencies a) E' b) E'' c) tan δ

E' showed a decrease along with increase of strain amplitude, which fits to the literature reports for rubber based on the Payne effect. (26) (27)

E'' and tan δ modulus values seem to decrease with increase of strain amplitude,. To further analyze this material response to strain amplitude the hysteresis loop cycle was analyzed over displacement and time as shown in Figure 29.

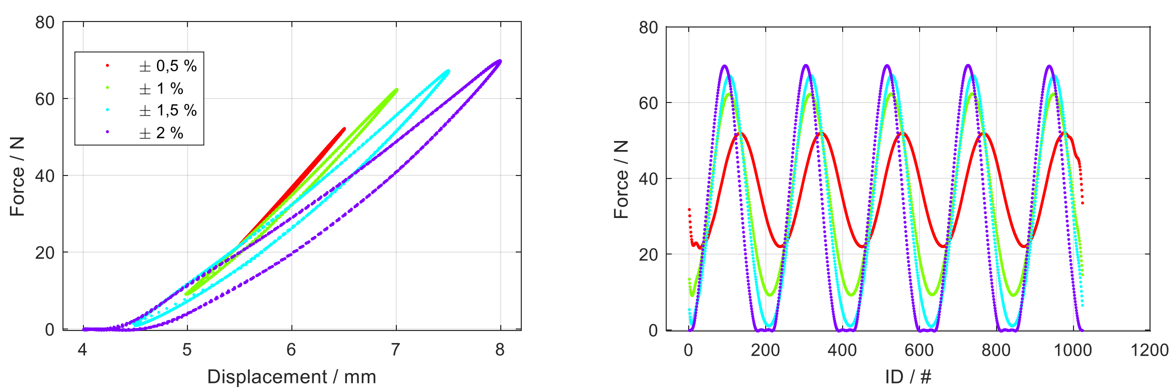

(a) (b)

Figure 29 – Hysteresis loops for different strain amplitudes over: a) displacement b) points taken throughout the test

The corresponding hysteresis loops in Figure 29 exhibit the strain amplitude dependence**.** Both area and slope seem to change substantially with increase of strain amplitude according to Figure 29 data. The dependence of hysteresis properties on strain amplitude is also reported in literature for rubber. (27) Furthermore, it was also observed that for the strain amplitude of ± 2% the PET material starts to buckle, which may suggest that this dynamic test's strain amplitude is too large for the PET 1440x2 cord. This buckling of the cord is seen in force plot as a measured force reaching values of zero.

At least one of the combinations of the test herein described and the one described in Subsection 4.2 share the same experiment conditions and the comparison of the values of the same testing conditions are shown in Figure 30.

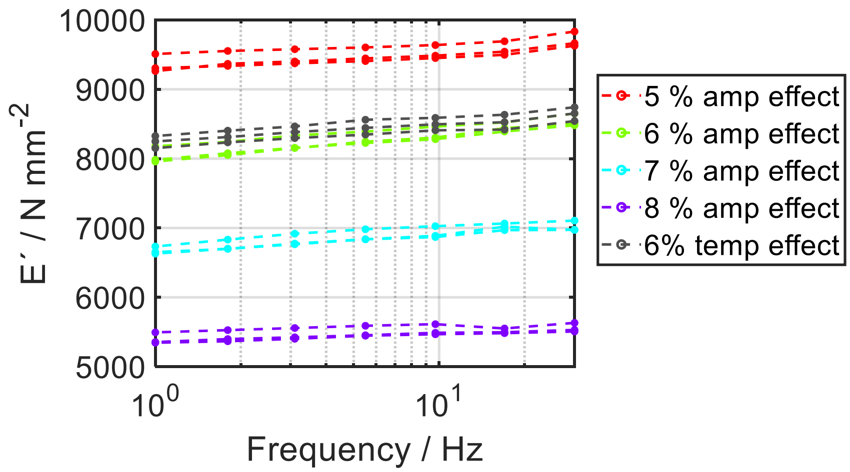

Figure 30 - E' versus frequency at different strain amplitudes comparison with results of Subsection 4.2.

The values of E' almost overlap for both tests which may indicate that the material responds the same way when subjected to the same conditions. This is an outcome that may be useful for the validation of the reliability of the procedures in this study: different procedures methods may lead to the same mechanical behavior for the tested material. Moreover, it may turn a good indicator of the accuracy of the data results.

4.5 Temperature monitoring of textile cords

The tests results of PET 630x2 and 2200x2 and Nylon 940x2 and 2800x2 are shown in Figure 31 and are grouped in Table 11.

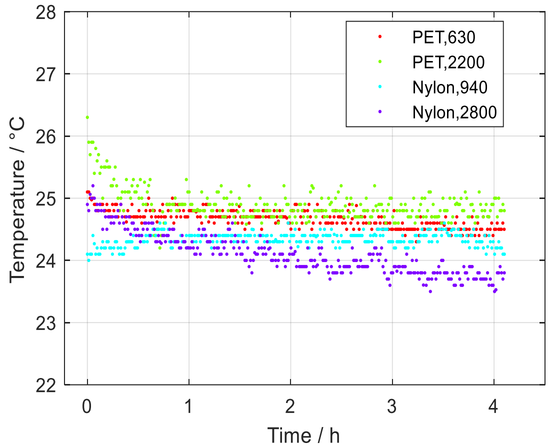

Figure 31 – Temperature monitoring data test over time for different material constructions

Thermal photos of a sample of PET 2200x2 were captured while being tested to verify cord´s temperature response. The results are shown in Figure 32.

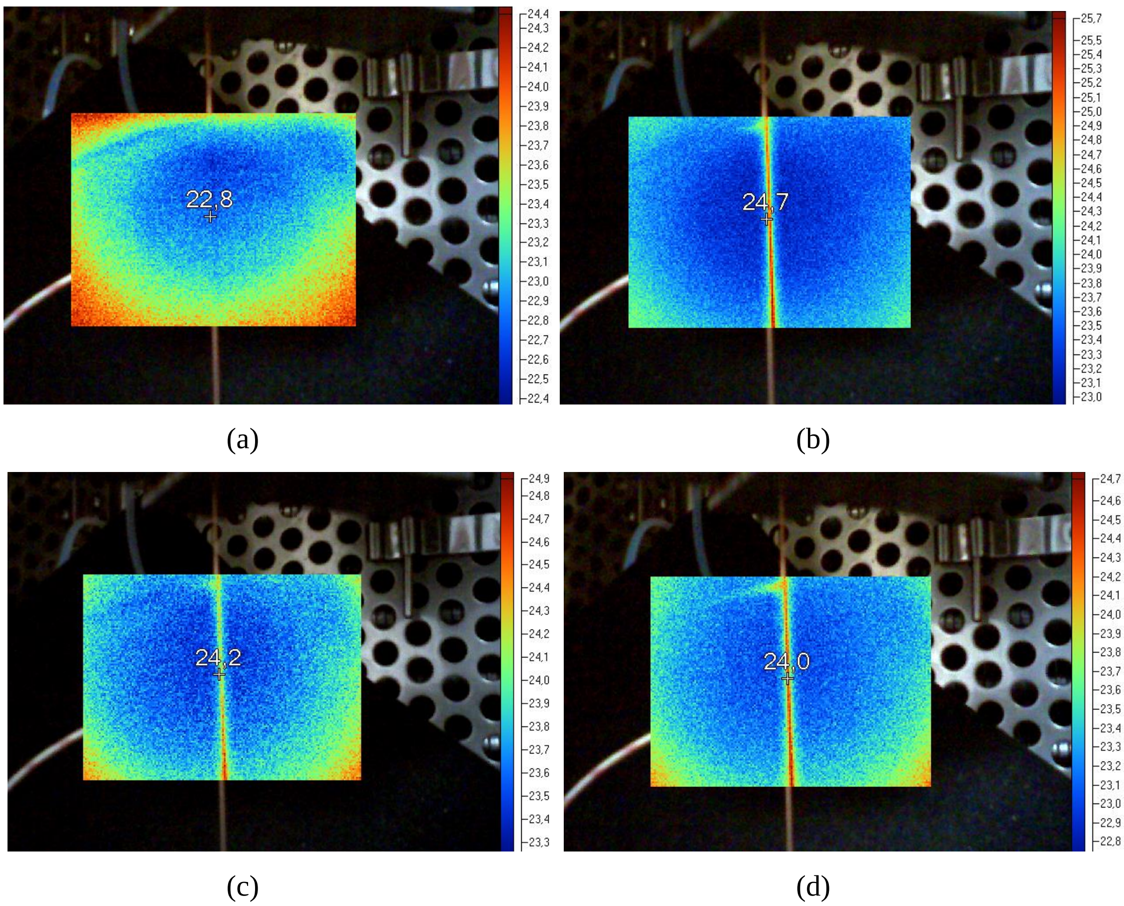

Figure 32 – Thermal photo captured of PET 2200x2 at a) 0 min b) 5 min c) 1 h d) 2h

Figure 32 shows a peak of temperature observed within 5 min of test followed by a decrease of temperature throughout the test, fitting with the trend of the temperature monitoring data shown in Figure 31.

Figure 31 also suggests that temperature for the same material at higher dtex shows more variation of temperature throughout the test, which is consistent with data presented in Table 11.

Table 11 - Temperature of different material constructions

Material construction	T initial / °C	Min T / °C	Max T / °C	Range / °C
PET 630	24,3	24,3	25,1	0,8
Nylon 940	24,2	24	24,6	0,6
PET 2200	24,9	24,2	26,3	2,1
Nylon 2800	23,7	23,5	25,2	1,7

In fact, PET 2200x2 and Nylon 2800x2 present range values of temperature, respectively, of 2.1 and 1.7 °C and PET 630x2 and Nylon 940x2 only shown a range of 0,8 and 0,6 °C. This may indicate that the higher density PET cord response generated more heat than the lower dtex cords.

Results of E' and tan δ over time are grouped in Figure 33.

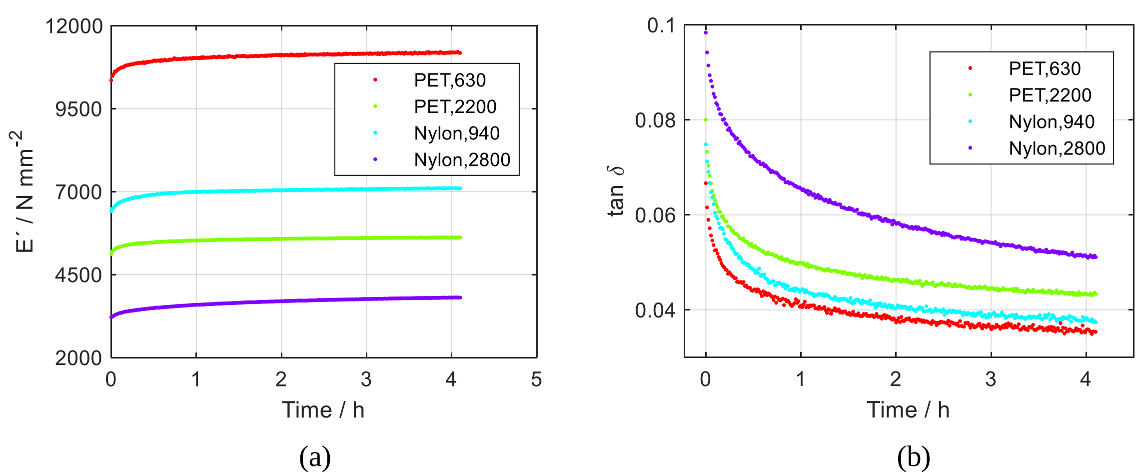

Figure 33 - Modulus over time for different material constructions a) E' b) tan δ

Figure 33 also may suggest that higher dtex materials experience higher energy loss, since tan δ values of PET 630 and Nylon 940 are lower than, respectively, PET 2200 and Nylon 2800. This increase of energy loss might be related to a higher amount of filament friction experienced in higher dtex cords. The hysteresis plots from the beginning and end for each material construction test are shown in Figure 34 and seem to fit with this possibility.

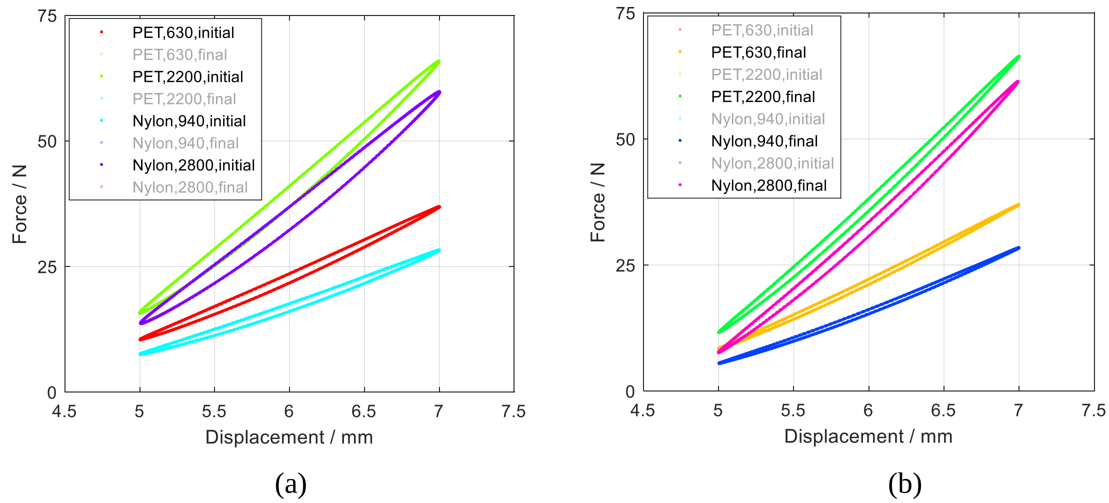

Figure 34 - Hysteresis for each material construction a) first cycle b) last cycle

In fact, both PET 2200x2 and Nylon 2800x2 showed a higher hysteresis slope and area when compared, respectively, to PET 630x2 and Nylon 940. Furthermore, Figure 34 also may suggest that slope seem to change slightly and area seem to change significantly throughout the test, which is consistent with the changes observed of E' and tan δ over time shown in Figure 33.

It is expected that higher frequencies show higher range of temperature experienced throughout the test. In order to further investigate this assumption, PET 2200x2 was also tested at 30 Hz as described in Subsection 3.2.5 and the results are shown in Figure 35.

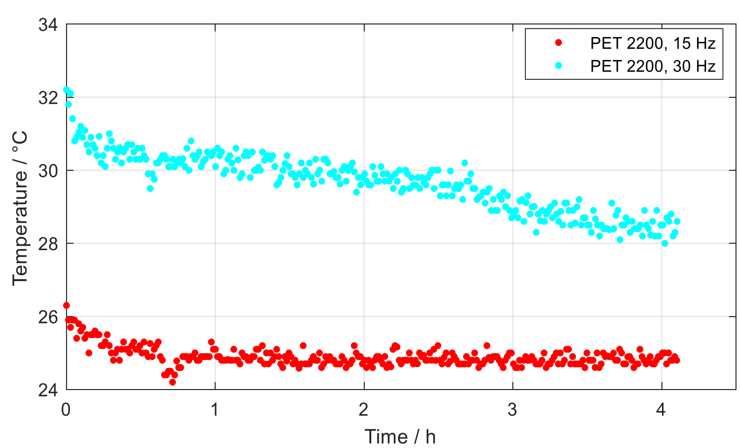

Figure 35 - Temperature monitoring data test over time for PET 2200x2 at 15 and 30 Hz.

Frequency of 30 Hz experienced a higher range of temperature than 15 Hz. Noteworthy, this higher increase of temperature might be appealing to study once it seems to display a substantial change in the temperature´s cord response.

5 Conclusions

This thesis provided information on the hysteresis of tire textile reinforcements, focusing on PET under static and dynamic conditions.

Stepwise relaxation test indicates the possibility of a dependence on temperature and all materials experienced material softening and temperature seems to influence overstress. In addition, increase of strain lead to an increase of stiffness. It was also possible to observe that different materials responded in a similar way for different temperatures and that these temperatures that shared the same material response were different for different materials. Dynamic tests seem to indicate that there is a dependence of the hysterical properties of PET 1440x2 on temperature and that the reinforcements soften along with temperature, which fits with the stepwise relaxation test results. It was also possible to observe thermal polymer transitions that seem to influence the material behaviour response while being stressed. Stiffness increased with pre-deformation, but the amount of hysteresis given by the loss modulus did not seem to be substantial enough for the pre-deformation range from 5% to 8% evaluated. The storage modulus decreased, and the amount of hysteresis increased with strain amplitude. In addition, ± 2% dynamic test strain amplitude was too high for PET 1440x2, causing the buckling of the cord. Noteworthy, different dynamic tests show similar results in similar conditions, which may be a good indicator of the replicability of the tests.

Differences between temperature variation for PET and nylon were observed in this work, under dynamic conditions. For higher dtex PET and nylon materials, a higher amount of hysteresis was detected, experiencing more energy loss and higher variation of temperature. Also, small changes of the amount of hysteresis throughout the dynamic test were observed, consistent with the possibility of the low loss modulus change and hysteresis loop evaluation of the PET 630x2, PET 2600x2, Nylon 940x2 and Nylon 2800x2.

The outcome of the dynamic mechanical analysis tests fits with the stepwise relaxation tests' results and seems to reveal a dependence of the hysteresis' modulus on temperature, frequency, pre-deformation and strain amplitude. Furthermore, a master curve was constructed with key importance for future projects, giving valuable information about the modulus variables under a higher range of frequencies than the measured by the MTS machine. For confidentiality reasons, the obtained master curve is not disclosed in this document. Finally also a test procedure was developed that seems promising for future works in order to have a better insight about the temperature changes of textile reinforcement cords under dynamic conditions.

6 Assessment of the work done

6.1 Objectives achieved

Until recently the hysteresis properties of rubber have been the motivation of several studies. This project provides an understanding on the viscoelastic and hysteresis phenomenon of textile reinforcement cords, mainly for PET. Textile reinforcement cords showed mechanical properties dependence on temperature, frequency, pre-deformation and strain amplitude. In addition, it was possible to investigate the temperature variation of textile cords under dynamic conditions for same materials at different linear densities. This was accomplished by:

- Implementation and optimization of a stepwise relaxation procedure for PET 1440x2, Nylon 470x2 and Hybrid 1680 + 1400 material constructions that allowed a better understanding of their response behavior and their temperature dependence.

- Implementation and development of dynamic test procedures for PET 1440x2 that provided insight about its dynamical properties and hysteresis behavior with temperature, frequency, pre-deformation and strain amplitude. Furthermore, a master curve was constructed with key importance for future projects. A wider range of pre-deformation can be investigated for a better perception of its effect on modulus.

- Implementation and development of a test procedure for PET 630x2, PET 2200x2, Nylon 940x2 and Nylon 2800x2, which allowed the evaluation of the cords' temperature and some dynamical properties and hysteresis behavior. In order to achieve evident statements regarding this study some procedure optimization can be done, which are contained in the following Subsection 6.2.

6.2 Limitations and future work

The novel results of this project are highlighted by scarcity of information available in the reported literature on the application of the DMA technique to textile reinforcement cords. Limitations relate mainly to time necessary to extended testing time for some of the trials needed to further clarify the results and their practical implications. MTS Acumen is not usually used in this type of dynamic evaluation, and it was also quite difficult and time-consuming to answer some unexpected technical issues and to deal with machine keep in check, regarding resonance and measurement resolution.

Given the novel aspect of this technique when applied for textile reinforcements, these studies are mainly preliminary, in order to obtain an overall intuition of how the cord behaves and what factors may have a relevant effect on its hysteresis. Being as so, several further studies are recommended, not only to obtain additional information but also as improvements to the current configuration. Some possible further research related to this this project are proposed as shown in Figure 36.

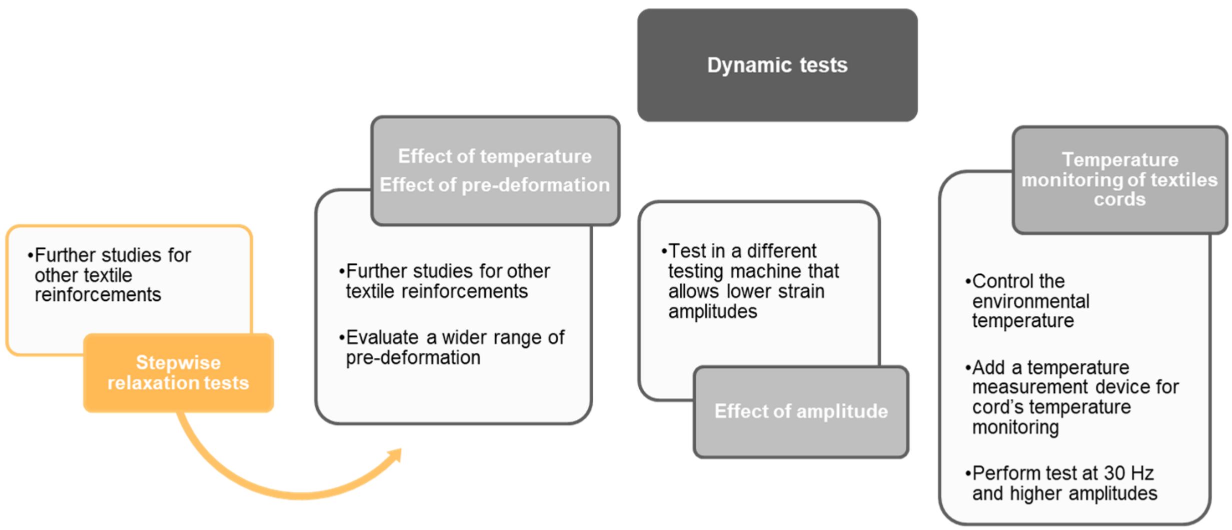

Figure 36 - Further investigations related to this this project for each study

For both stepwise relaxation and effect of temperature and effect of pre-deformation studies additional textiles reinforcements should be performed.

For the effect of pre-deformation study a wider range of pre-deformation may be evaluated. In this study the range of pre-deformation was only from 5 to 8 %, which did not lead to a substantial change in the stiffness of the PET cord. A wider range of pre-deformation is likely to have a greater impact on the hysteresis properties.

Lower strain amplitudes investigation may also be performed and for that a different testing machine should be used, since the MTS machine does not allow lower strain amplitudes within the range studied due to resolution issues.

For the temperature monitoring of textiles cords each material tested started with a different initial temperature. Due to MTS process limitations, it was not possible to control simultaneously the temperature environment and the temperature of the cords. A feasible optimization of the procedure may consist of implementing an additional measurement device to record the temperature of the cords samples and use MTS machine to control the environment´s temperature. Also, for a higher increase in the range of temperature experienced by the textile reinforcements cords throughout the test, both higher frequencies and strain amplitudes may be performed, which may lead to a more distinct effect on the hysteresis properties.

Further studies are warranted, not only to obtain additional evidence but also as improvements to the current configuration:

- Application and optimization of the test procedure for other reinforcement materials, such as rayon and hybrid.
- Consideration of a force-controlled test mode, as an alternative to the currently used strain-control, which possibly would allow better improved parameters calculated by the MTS machine.

6.3 Final assessment

It was very important the development of this master thesis in an industry environment once it gave me the opportunity to learn a lot about things that cannot be perceived at the University. Working in this environment also gave me analysis competences and new abilities to overcome practical problems.

Textile reinforcements field is very interesting and allowed me to apply my knowledge on polymer materials and materials structure. This work provided me a new insight about the behavior of the textile materials and may have initiated a way to further related projects to pursue in Continental. Indeed, this project allowed me a better understanding of the behavior of some textile reinforcements and their purpose in pneumatic tires.

At the end I have grown in both personal and professional level and I am thankful for each person that contributed and was part of this experience.

References

(1) Continental Reifen Deutschland GmbH, “Continental Corporation - Facts & Figures,”[Online] Available at https://www.continental-tires.com/car/company/about-us/corporate. (Accessed September 2018).

(2) Continental Reifen Deutschland GmbH, “Employee key figures and structure,”[Online] Available at https://www.continental-corporation.com/en/sustainability/employees/employee-key-figures-and-structure-63366. (Accessed September 2018).

(3) Continental Reifen Deutschland GmbH, “Continental at a Glance – Key Facts,” [Online] Available at https://www.continental-corporation.com/en/career/working-at-continental/ your-employer/continental-at-a-glance. (Accessed September 2018).

(4) M. Gomes, “Hysteresis in Tyre Textile Reinforcements”, 2018.

(5) Continental Reifen Deutschland GmbH, “Course Catalogue – 06 Reinforcements” [Online] https://tireacademy.conti.de/mod/iccoursemgmt/catalog.php?id=17. (Accessed October 2018).

(6) Continental Reifen Deutschland GmbH, “Tyre Basics - Passenger Car Tyres”, 2013.

(7) G. Wahl, “Basics of Textile Reinforcement Materials for Tires Content, ed. Continental”, 2016.

(8) Continental Reifen Deutschland GmbH, “Course Catalogue – 05 Construction” [Online] https://tireacademy.conti.de/mod/iccoursemgmt/catalog.php?id=17. (Accessed October 2018).

(9) Mukhopadhyay S. K., Partridge J. F., “Automotive textiles”, Textile Progress, 29, 1-125, 1999.

(10) Shingo F., "Effect of material properties on tire performance characteristics”, tire science and technology, Part I, TSTCA, 15, 198-206, 1987.

(11) B. E. Lindenmuth, “An Overview of Tire Technology,” in The Pneumatic Tire, 2006, ch. 1.

(12) D. B. Wootton, The Application of Textiles in Rubber, 2001.

(13) AllroundLine Material-Prüfmaschine Aus Dem Hause ZwickRoell. [Online] https://www.zwickroell.com/de-de/universalpruefmaschinen/allroundline-material-pruefmaschine. (Accessed November 2018).

(14) Gent A. N., Walter J. D., “The pneumatic tire”, NHTSA, EUA, 2005.

(15) B. Rodgers and W. Waddell, “Tire Engineering,” Sci. Technol. Rubber, 2013.

(16) G. Burrowes, “Reinforcing materials in rubber products”, Nokian Tyres PLC, U.S.A, 2010.

(17) D. B. Wootton, The Application of Textiles in Rubber, 2001.

(18) E. T. McDonel, “Tire Cord and Cord-to-Rubber Bonding,” in The Pneumatic Tire,2006, ch.3.

(19) A. Louis, J. W. M. Noordermeer, W. K. Dierkes, and A. Blume, “Technologies for Polymer Cord / Rubber Adhesion in Tire Applications,” Proceedings of 186th Technical Meeting ACS Rubber Division, 2014.

(20) Continental Reifen Deutschland GmbH, “Course Catalogue – 01 Tire Onboarding Fundamentals” [Online] https://tireacademy.conti.de/mod/iccoursemgmt/catalog.php?id=17. (Accessed October 2018).

(21) Wollscheid, D., and A. Lion. “The Benefit of Fractional Derivatives in Modelling the Dynamics of Filler-Reinforced Rubber under Large Strains: A Comparison with the Maxwell-Element Approach.” Computational Mechanics, vol. 53, no. 5, May 2014, pp. 1015–31.

(22) M. A. Meyers and K. K. Chawla, Mechanical Behavior of Materials, 2nd ed. Cambridge University Press, 2009.

(23) DIN 53513:1990-03, Prüfung von Kautschuk und Elastomeren; Bestimmung der viskoelastischen Eigenschaften von Elastomeren bei erzwungenen Schwingungen außerhalbder Resonanz. Deutsches Institut für Normung, 1990.

(24) “Klimaprüfschränke der Baureihe KPK KH.” mytron Bio- und Solartechnik GmbH, [Online] https://www.mytron.de/produkte/klimapruefschraenke-der-baureihe-kpk-kh/. (Accessed November 2018).

(25) Perkin Elmer, “Dynamic Mechanical Analysis Basics: Part 2 Thermoplastic Transitions and Properties”, 2007.

(26) Wollscheid, D., and A. Lion. “Predeformation- and Frequency-Dependent Material Behaviour of Filler-Reinforced Rubber: Experiments, Constitutive Modelling and Parameter Identification.” International Journal of Solids and Structures, vol. 50, no. 9, May 2013, pp. 1217–25.

(27) Rendek, Martin, and Alexander Lion. “Amplitude Dependence of Filler-Reinforced Rubber: Experiments, Constitutive Modelling and FEM – Implementation.” International Journal of Solids and Structures, vol. 47, no. 21, Oct. 2010, pp. 2918–36.

Appendix A – Context and State of art

Table 12 - Materials of PLT tire components and their main functions (7)

#	Component	Material	Function:
1	Bead Core	Rubberized steel cord wires	Ensures the connection of the tire with the rim
2	Apex (Filler)	Synthetic rubber	Influences steering precision, driving stability and damping comfort
3	Inner liner	Rubber blend, containing Halo-butyl and optional platy fillers	Improves air retention by lowering permeation outwards through the tire Allows longer, more practical service intervals Influences durability and noise/ vibration/ harshness issues, Withstands high shear strain stresses in very small sidewall heights
4	Carcass Ply	Layer(s) of rubberized textile cords (Rayon/ Polyester) in radial direction (86°/90°)	Carries most of the load caused by the inner pressure of the tire Connects the bead with the crown area and thereby transmitting tension forces between these two areas
5	Bead reinforcement	Layer of rubberized textile / steel cords (Rayon/ Nylon/ PET) under a specific angle (45°/60°)	Stiffens the lower sidewall/ bead area to influence the driving behavior and the high speed durability
6	Rim strip	Synthetic rubber	Ensures the correct seating of the tire on the rim Stiffens the lower bead area especially with a rim protection rib Improved resistance to abrasion from the rim
7	Sidewall	Rubber blend, often high natural rubber content	Protects the carcass against direct mechanical load (curbstones) and environmental conditions (O3), influences force transmission (and thereby driving behavior), withstands high shear strain stresses in very small sidewall heights

8	Belt (Breaker)	Minimum two layers of calendared steel cord under a specific angle (22°- 36°) - reversed between the belts	Stabilizes the crown area of the tire and transmit forces from the contact patch to the carcass, influences the driving stability and the durability of the tire
9	Cap ply	Rubberized textile cords (Nylon/ Hybrid/Polyester) 10 or 15mm strips wound around the belts	Stiffness of belt package and restriction of circumferential forces are influenced by the selection of cap ply fabric and layup pattern Controls the static and dynamic contour of the tire, which affect geometric measurements, high speed capability and footprint shape
10	Tread	Synthetic and natural rubber, multiple layers (cap/ base/ wing)	Compound: Influences wear, grip, rolling resistance and electrical conductivity Pattern: Influences aquaplaning, noise and handling properties

Appendix B – Results and Discussion

B.1 Effect of temperature on stiffness at fully relaxed state

Table 13 - Number of samples for each temperature for each material tested

	Temperature / °C				
	23	40	80	110	160
Nylon	3	2	4	3	3
Hybrid	3	3	3	3	3
Polyester	3	2	3	4	2

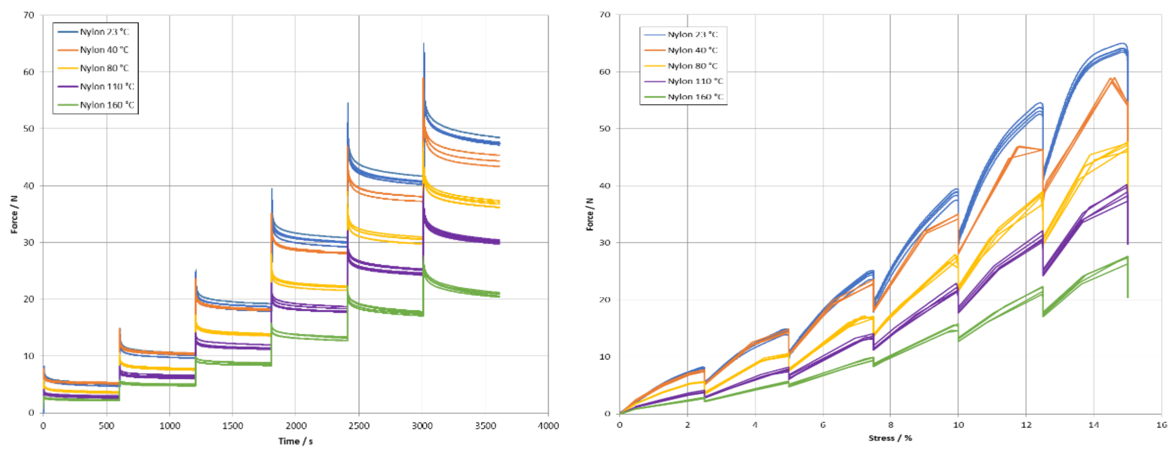

a) b)

Figure 37 - Nylon 470x2 at different temperatures for all samples a) Force versus time b) Stress distribution

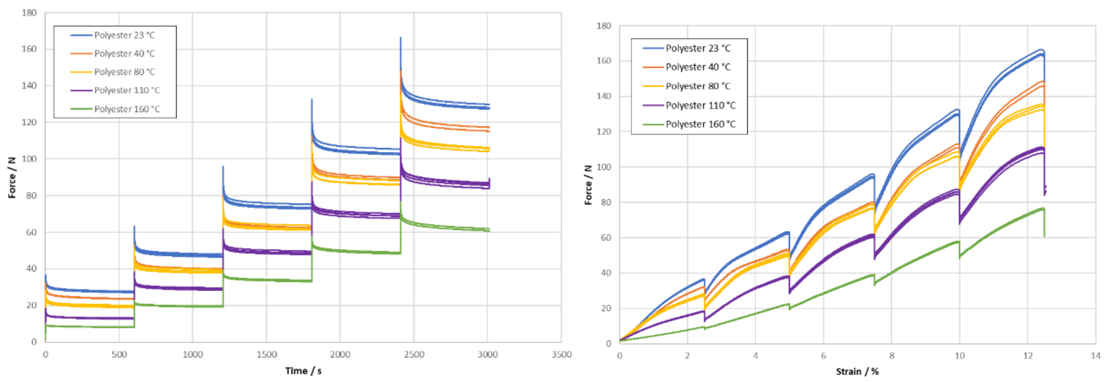

a) b)

Figure 38- PET 1440x2 at different temperatures for all samples a) Force versus time b) Stress distribution

Table 14 - Stress variation in each relaxation strain steps at different temperatures for Nylon 470x2

Δ Stress / MPa		ε / %				
		2,5	5	7,5	10	12,5
Temperature / °C	23	22,9	31,4	39,7	58,7	90,0
	40	19,0	21,3	39,6	52,9	67,8
	80	16,7	21,8	24,4	30,5	43,5
	110	8,9	12,4	13,5	20,5	32,1
	160	4,8	6,0	9,1	15,9	28,7

Table 15 - Stress variation in each relaxation strain steps at different temperatures for Hybrid 1680 +1400

Δ Stress / MPa		ε / %p				
		2,0	4,0	6,0	8,0	10,0
Temperature / °C	23	20,7	32,6	65,0	115,4	181,2
	40	17,4	28,9	54,1	97,5	155,2
	80	16,4	25,4	46,4	115,4	124,0
	110	9,9	17,0	35,8	80,5	105,9
	160	5,5	9,3	24,3	68,6	99,0

B.2 Effect of temperature at a wide range of frequency

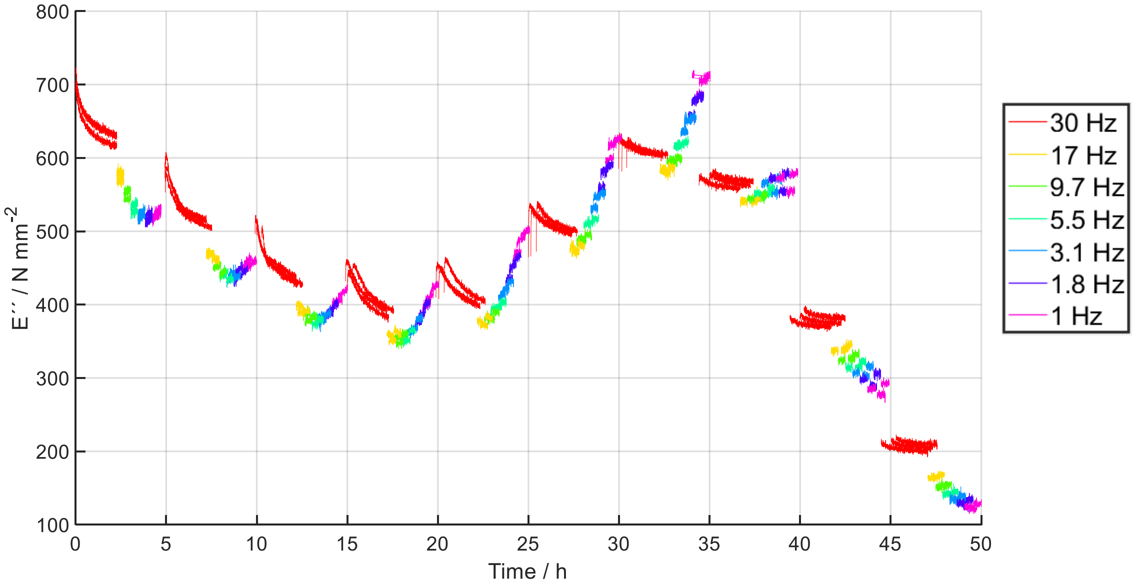

(a)

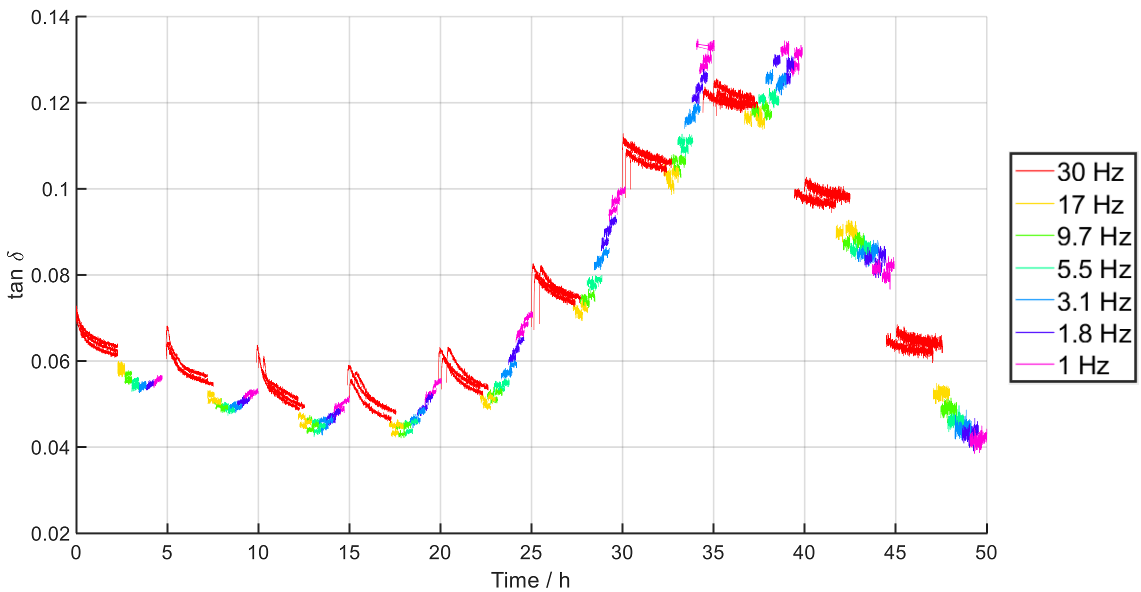

(b)

Figure 39 - Frequency sweeps nested in temperature sweep for three samples a) E'' over time b) tan δ over time

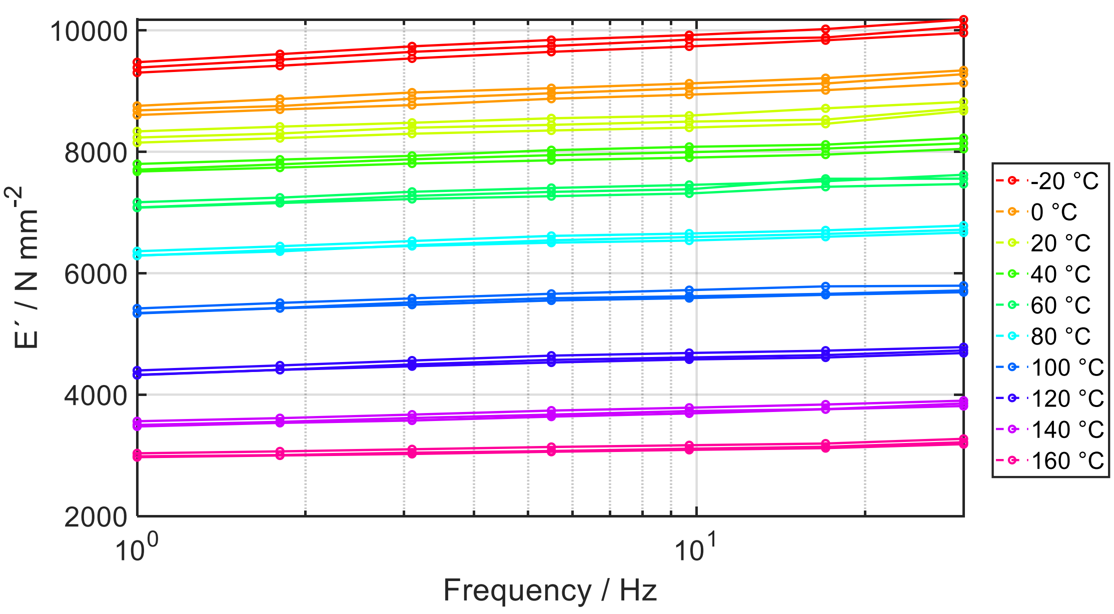
10000
8000
6000
4000
2000
E´ / N mm-2
10^0
10^1
Frequency / Hz
-20 °C
0 °C
20 °C
40 °C
60 °C
80 °C
100 °C
120 °C
140 °C
160 °C

(a)

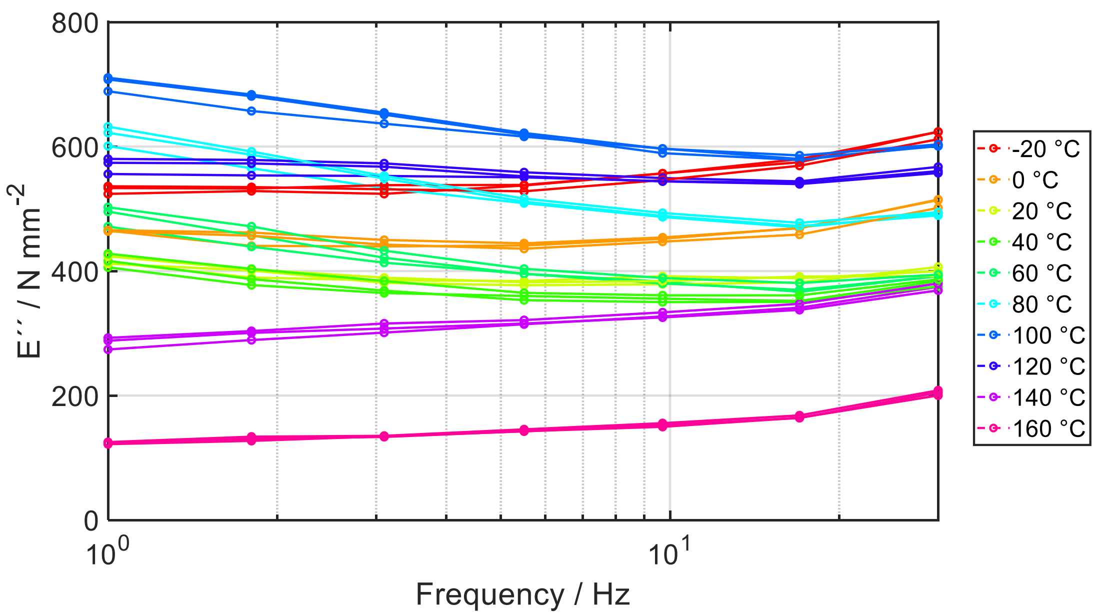
800
600
400
200
0
E´´ / N mm-2
10^0
10^1
Frequency / Hz
-20 °C
0 °C
20 °C
40 °C
60 °C
80 °C
100 °C
120 °C
140 °C
160 °C

(b)

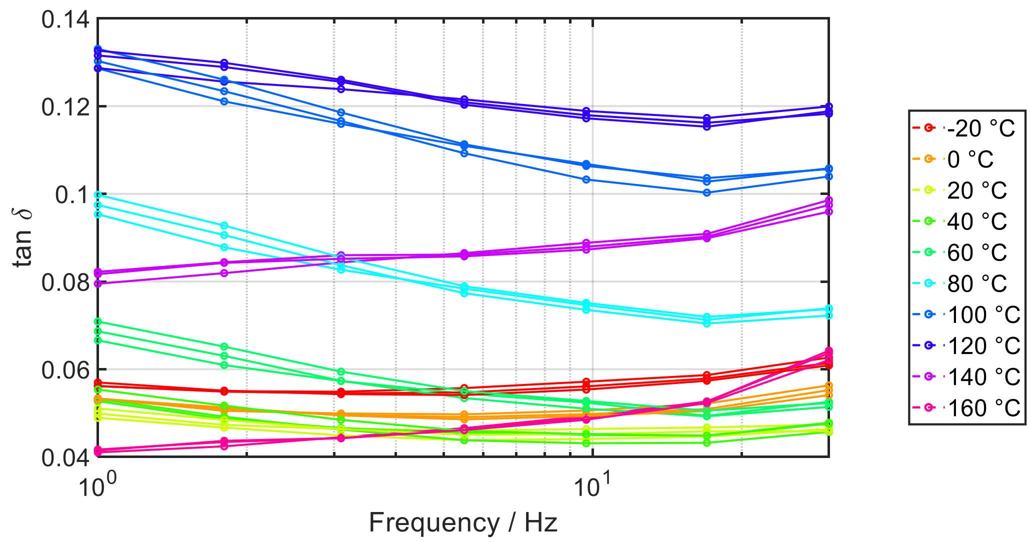

(c)

Figure 40 – Modulus predicted values over frequencies at different temperatures for three samples a) Force b) E'' c) tan δ

B.3 Effect of static pre-deformation at a wide range of frequency

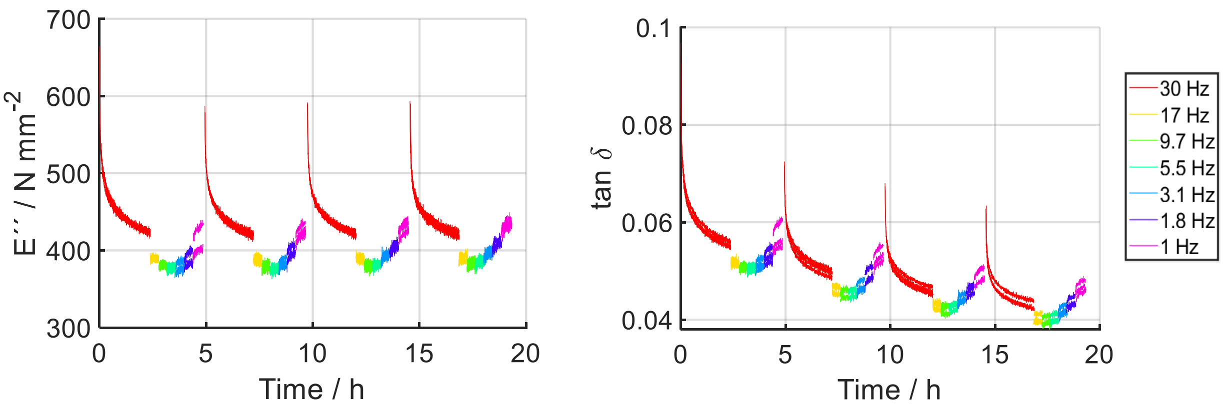

(a) (b)

Figure 41 - Frequency sweeps nested in pre-deformation sweeps for three samples a) E'' over time b) tan δ over time

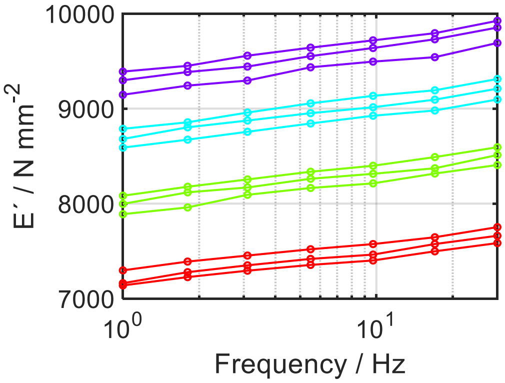

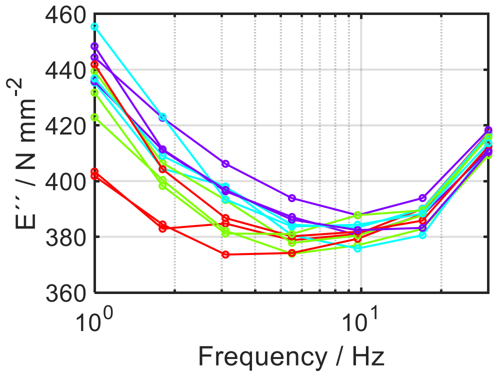

(a) *(b)*

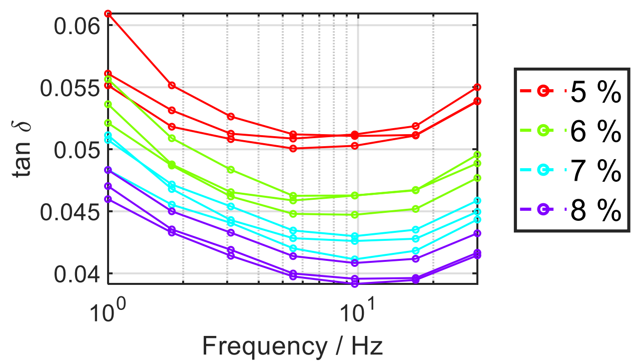

(c)

Figure 42 – Modulus predicted values over frequency at different pre-deformations for three samples a) E' b) E'' c) tan δ

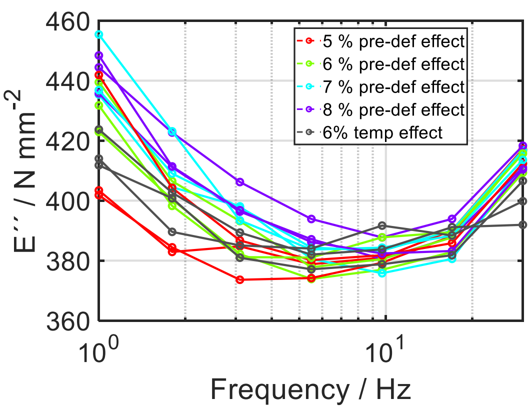

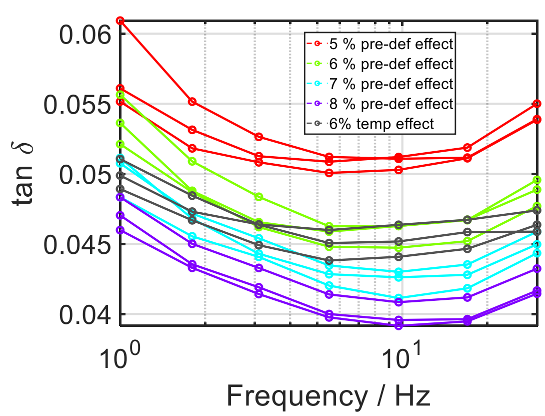

(a) (b)

Figure 43 - Modulus predicted values over frequency at different pre-deformations for three samples comparison with Subsection 4.2. a) E'' b) tan δ

B.4 Effect of strain amplitude at a wide range of frequency

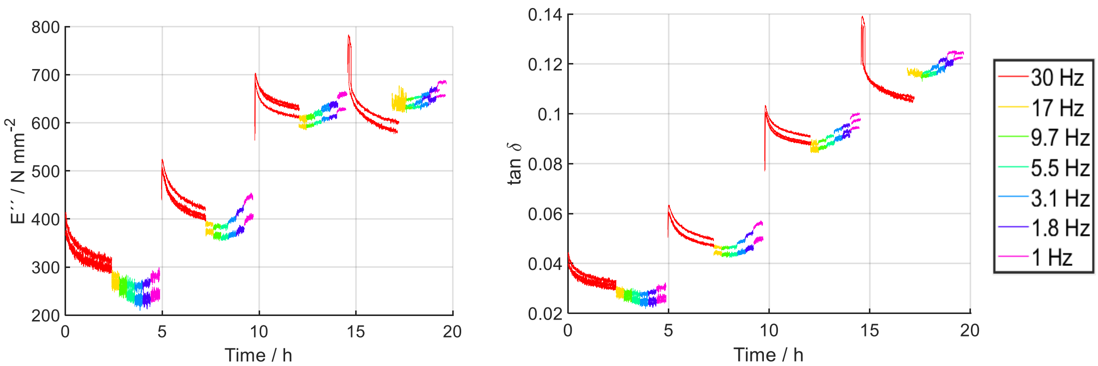

(a) (b)

Figure 44 - Frequency sweeps nested in strain amplitude sweeps for three samples a) E'' over time b) tan δ over time

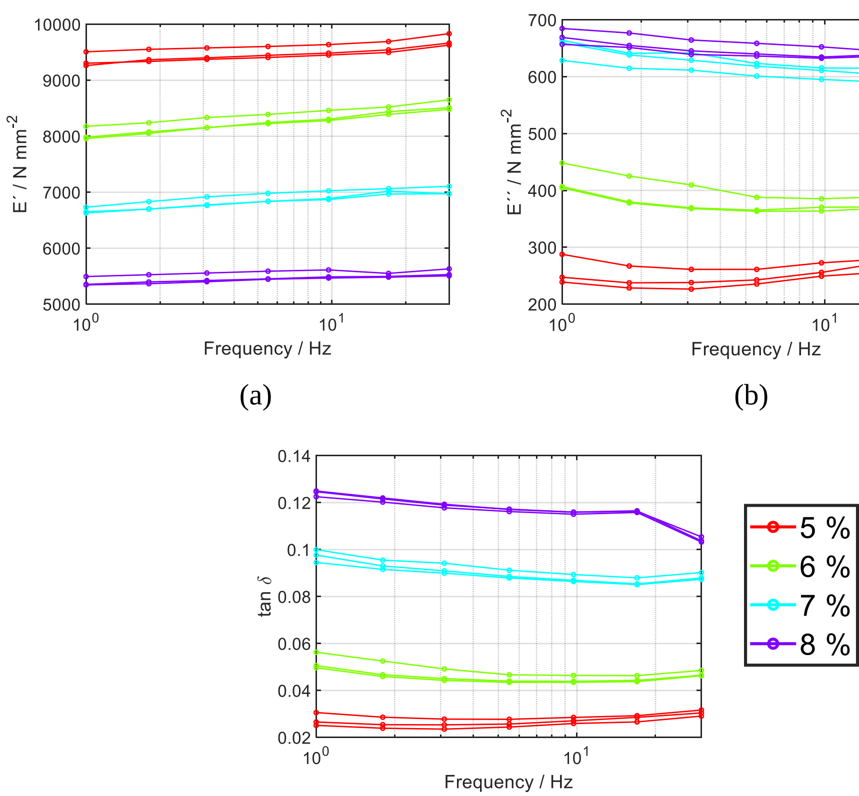

(a) (b)

(c)

Figure 45 - Modulus predicted values over frequency at different strain amplitudes for three samples a) E' b) E'' c) tan δ

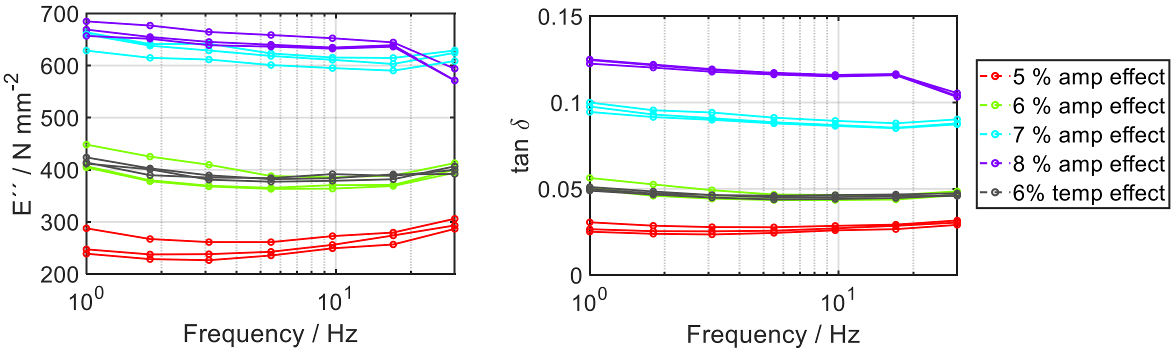

. (a) (b)

Figure 46 - Modulus predicted values over frequency at different strain amplitudes for three samples comparison with Subsection 4.2. a) E' b) E'' c) tan δ

B.5 Temperature monitoring of textile cords

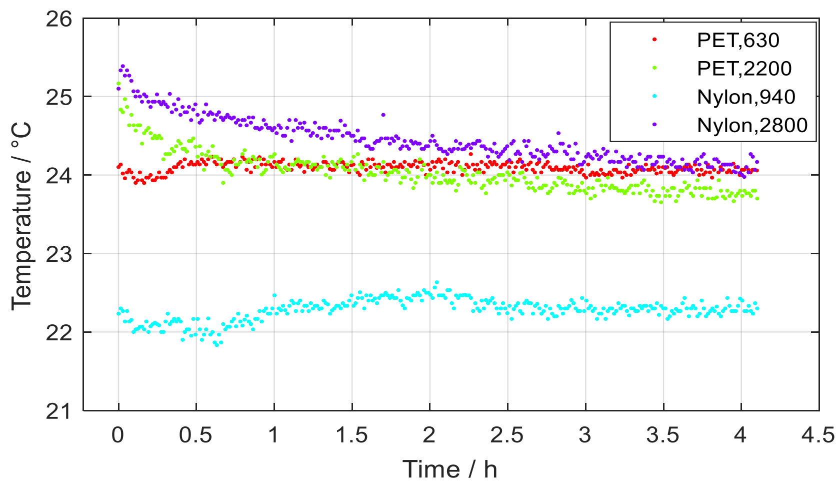

Figure 47 - Mean temperature monitoring data test over time for all material constructions samples

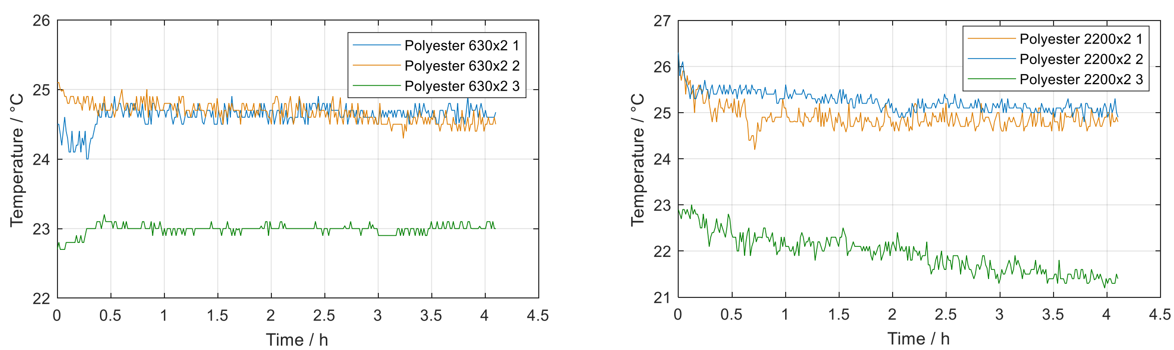

(a) (b)

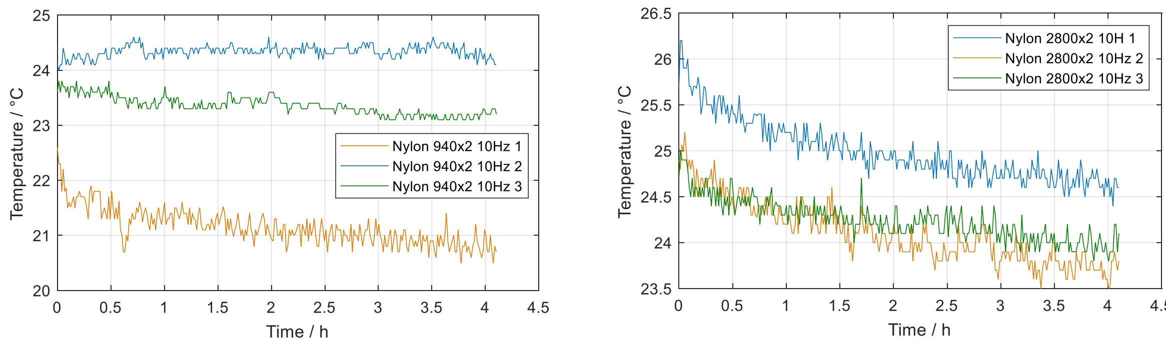

(c) (d)

Figure 48 - Temperature monitoring data test over time for all samples of different material constructions a) PET 630x2 b) PET 2200x2 c) Nylon 940x2 d) Nylon 2800x2

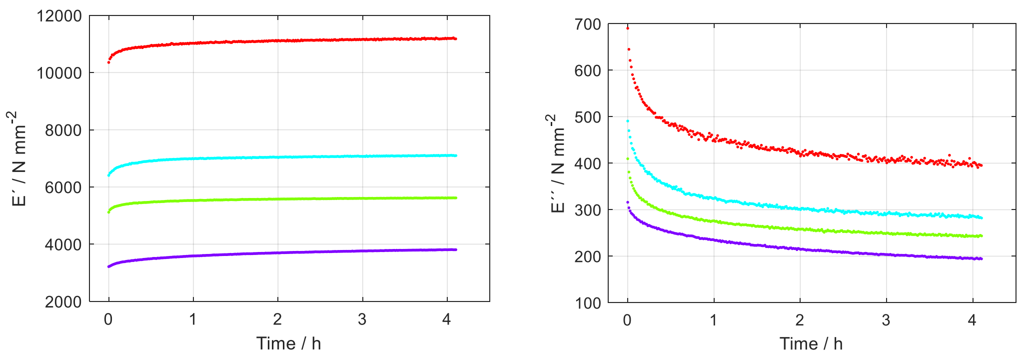

(a) (b)

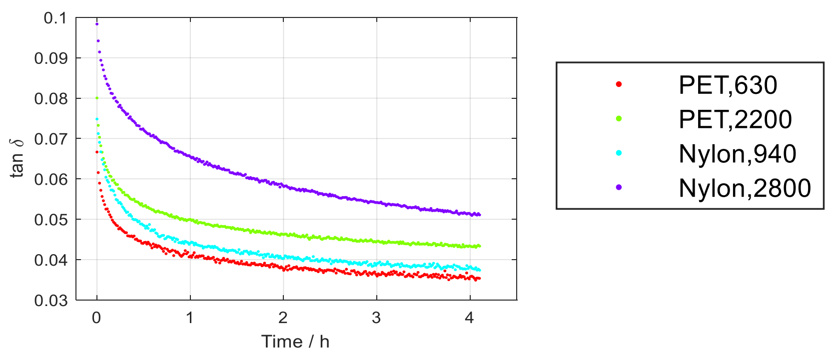

(c)

Figure 49 - Modulus over time for all different material constructions samples a) E' b) E'' c) tan δ

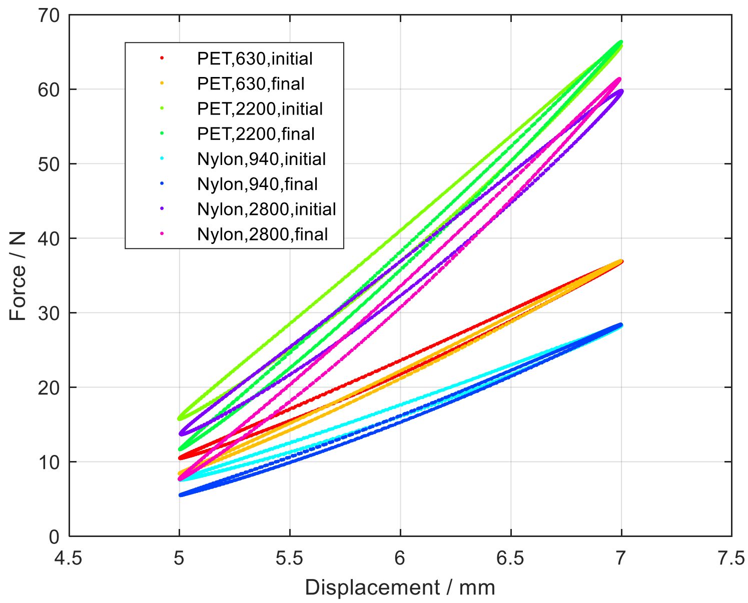

Figure 50 - Hysteresis for all material construction samples a) first cycle b) last cycle